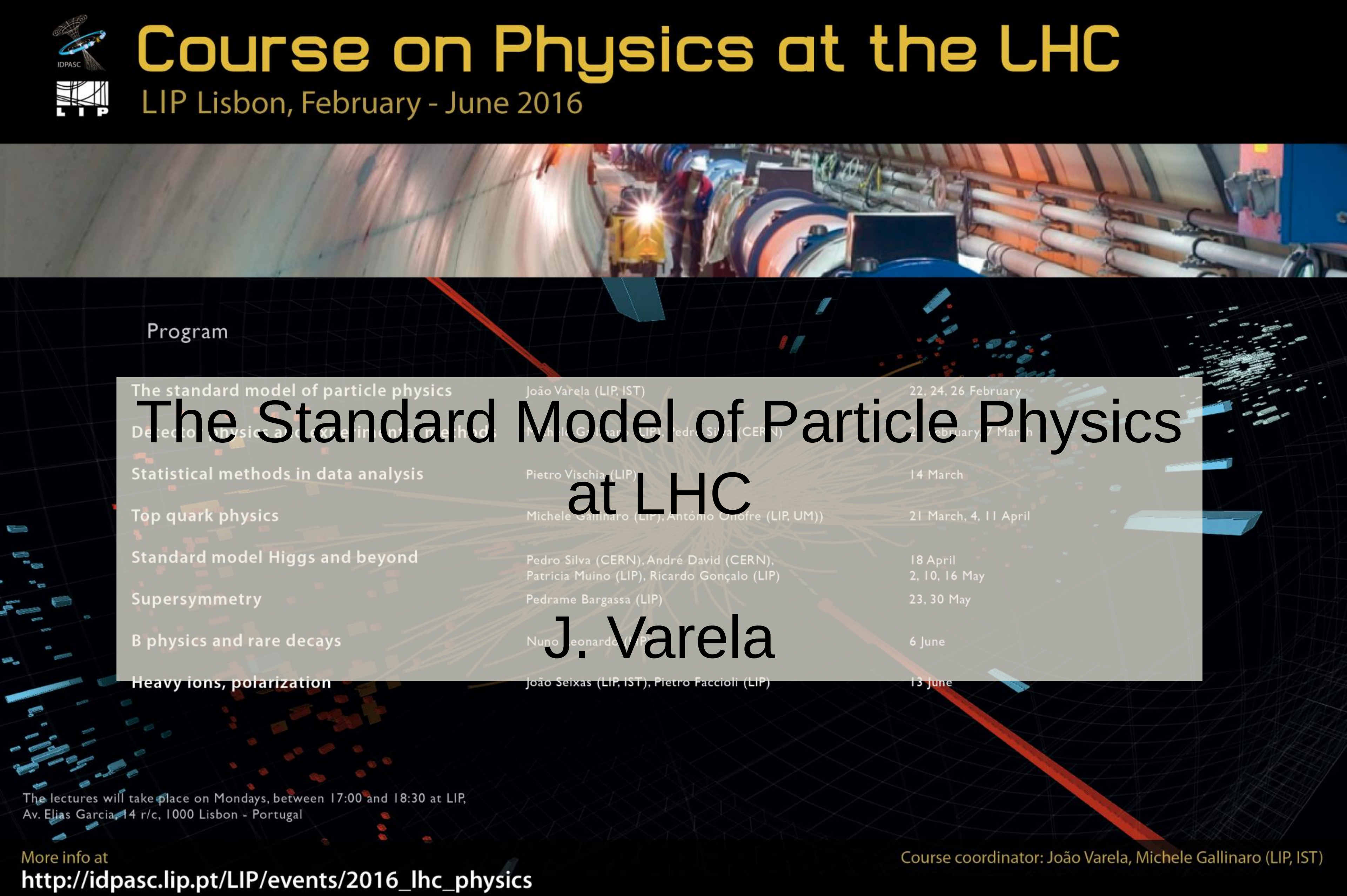

The Standard Model of Particle Physics at LHC

J. Varela

The Standard Model at LHC

1. Hadron interactions
2. QCD and parton densities
3. Monte Carlo generators
4. Luminosity and cross-section measurements
5. Minimum bias events
6. Jet physics
7. W and Z physics

Hadron Interactions

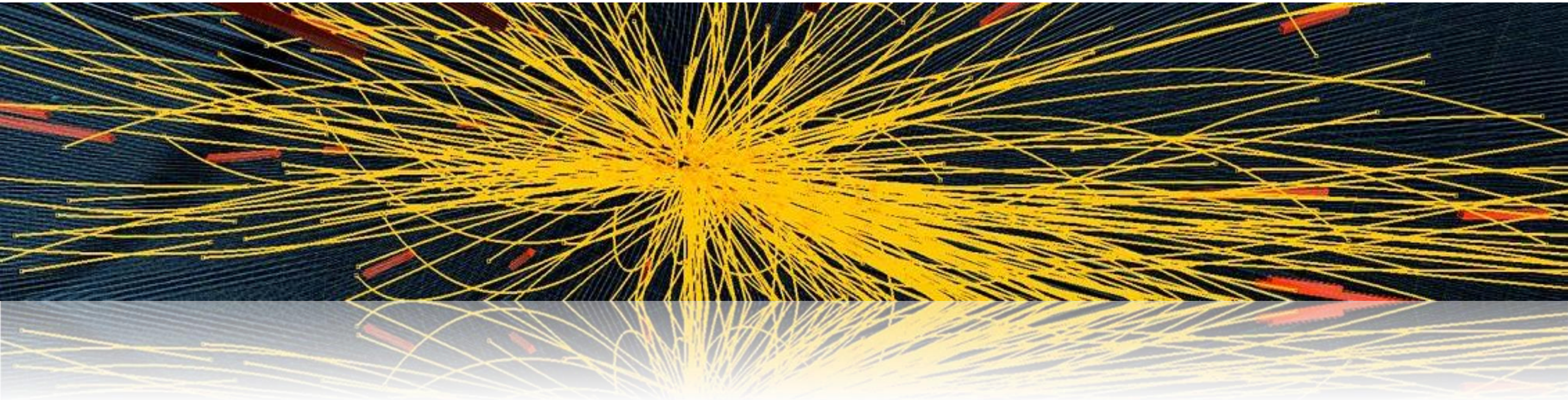

Kinematical variables

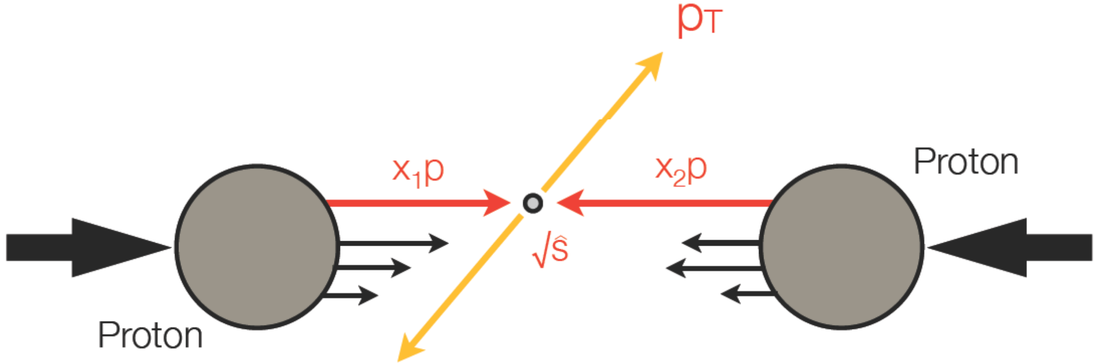

Schematic
proton-proton scattering

Relevant kinematic variables:

- Transverse momentum: p_T
- Rapidity: $y = ½ \cdot \ln (E-p_z)/(E+p_z)$
- Pseudorapidity: η = -ln tan ½θ
- Azimuthal angle: φ

Pseudorapidity

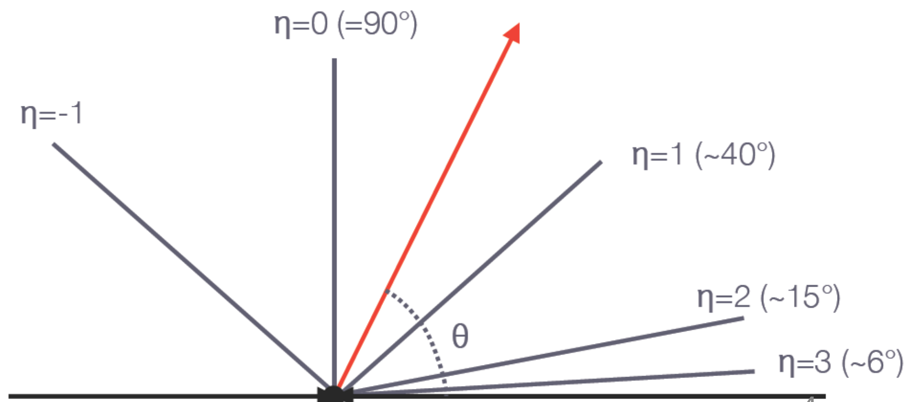

Invariant mass

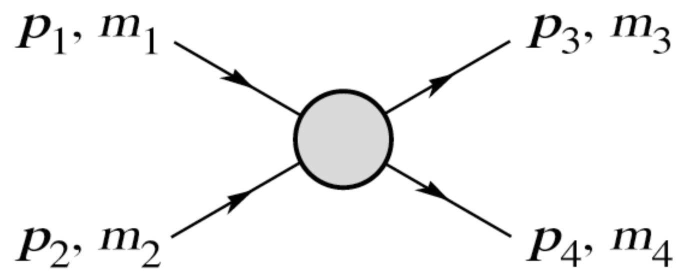

Invariant Mass:

$$M^2 = (p_1 + p_2)^2$$
$$= (E_1 + E_2)^2 - (\vec{p}_1 + \vec{p}_2)^2$$
$$= m_1^2 + m_2^2 + 2E_1E_2(1 - \vec{\beta}_1\vec{\beta}_2)$$

Center of mass energy

Center-of-mass Energy:

$$E_{\mathrm{cm}} = \left[(E_1 + E_2)^2 - (\vec{p}_1 + \vec{p}_2)^2\right]^{\frac{1}{2}}$$

Particle 2 at rest:

$$\sqrt{s} = \quad E_{\mathrm{cm}} = \left[m_1^2 + m_2^2 + 2E_1m_2\right]^{\frac{1}{2}}$$

Particle Collider:
$[E_1 = E_2;\ \vec{p}_1 = -\vec{p}_2;\ m_1 = m_2 \approx 0]$

$$E_{\mathrm{cm}} = 2E$$

Cross section
Matrix element
Phase space

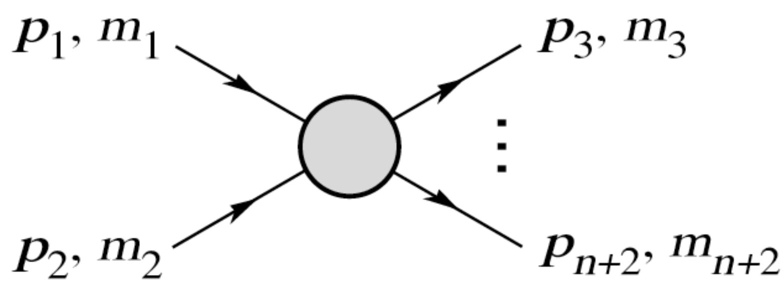

Differential
Cross Section:

Matrix element

$$d\sigma = \frac{(2\pi)^4 |\mathscr{M}|^2}{4\sqrt{(p_1 \cdot p_2)^2 - m_1^2 m_2^2}} \times \; d\Phi_n(p_1 + p_2;\; p_3, \ldots, p_{n+2})$$

n-body
phase space

$$d\Phi_n = \ldots$$

$$\ldots = \delta^4\left(P - \sum_{i=1}^{n} p_i\right) \prod_{i=1}^{n} \frac{d^3 p_i}{(2\pi)^3 2E_i}$$

with $P = p_1 + p_2$

Proton-Proton Scattering @ LHC

$$\sigma = \sum_{ij} \int dx_1 dx_2 \; f_i(x_1, Q^2)\, f_j(x, Q^2)\; \hat{\sigma}(Q^2)$$

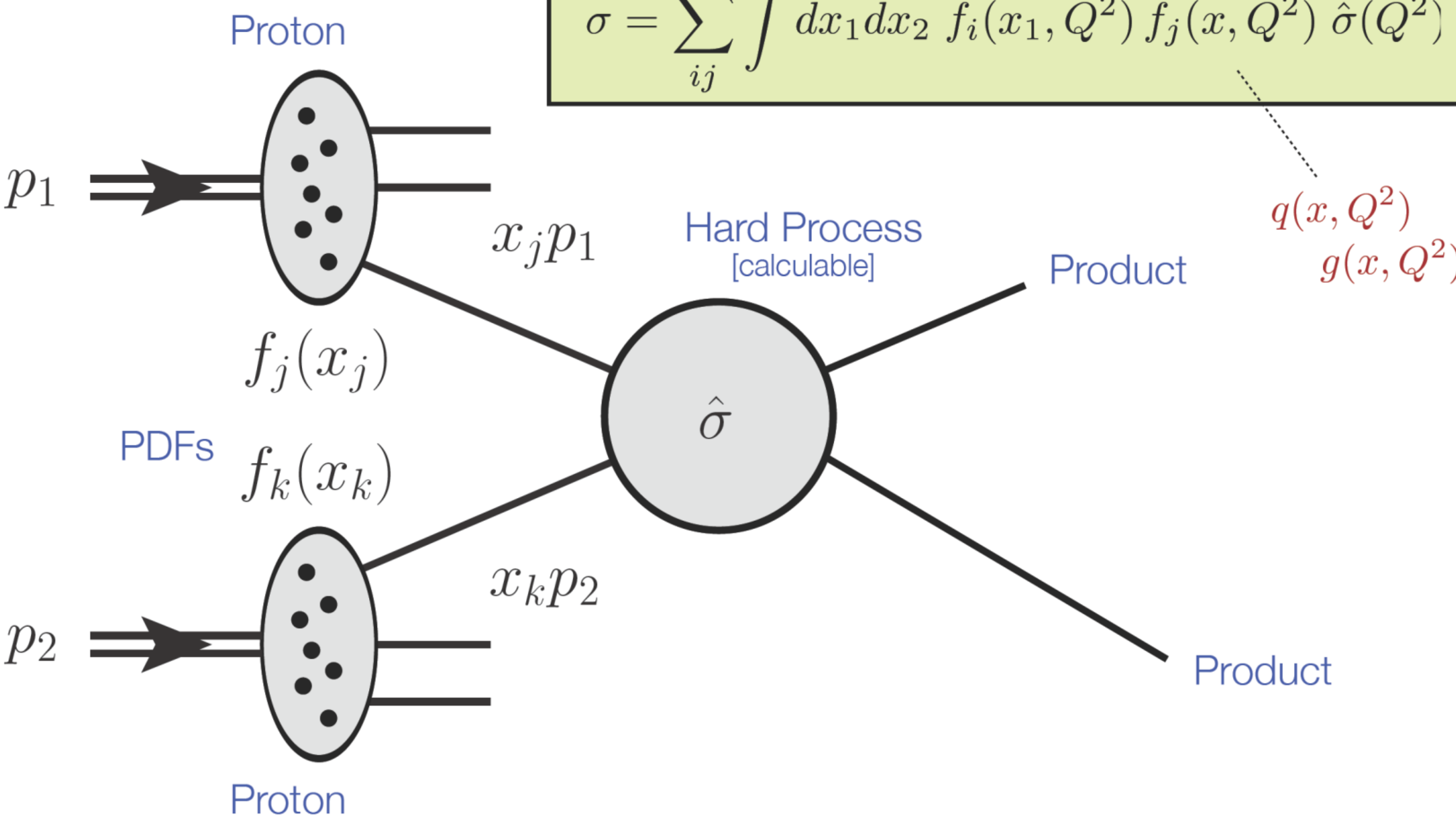

Example: Drell-Yan Process

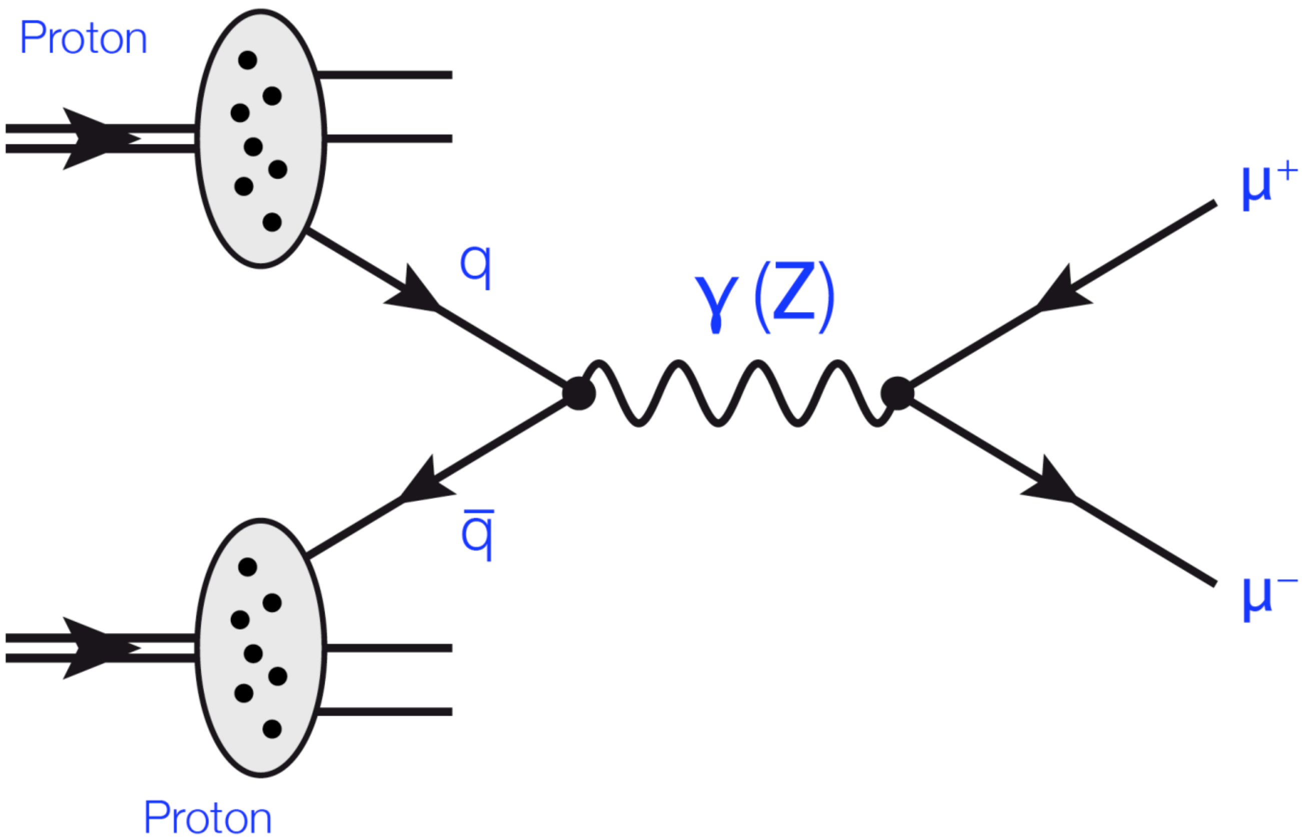

QCD Matrix Elements

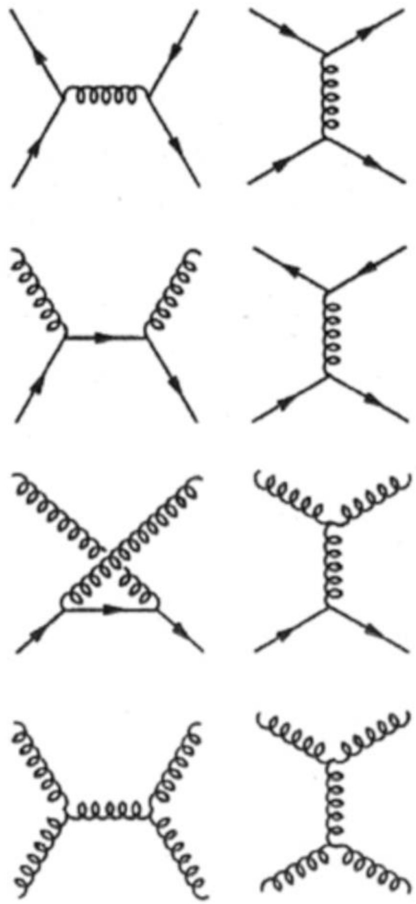

Subprocess	$\vert\mathcal{M}\vert^2/g_s^4$	$\vert\mathcal{M}(90^\circ)\vert^2/g_s^4$
$\left.\begin{array}{l} qq' \to qq' \\ q\bar{q}' \to q\bar{q}' \end{array}\right\}$	$\frac{4}{9}\frac{\hat{s}^2+\hat{u}^2}{\hat{t}^2}$	2.2
$qq \to qq$	$\frac{4}{9}\left(\frac{\hat{s}^2+\hat{u}^2}{\hat{t}^2}+\frac{\hat{s}^2+\hat{t}^2}{\hat{u}^2}\right)-\frac{8}{27}\frac{\hat{s}^2}{\hat{u}\hat{t}}$	3.3
$q\bar{q} \to q'\bar{q}'$	$\frac{4}{9}\frac{\hat{t}^2+\hat{u}^2}{\hat{s}^2}$	0.2
$q\bar{q} \to q\bar{q}$	$\frac{4}{9}\left(\frac{\hat{s}^2+\hat{u}^2}{\hat{t}^2}+\frac{\hat{t}^2+\hat{u}^2}{\hat{s}^2}\right)-\frac{8}{27}\frac{\hat{u}^2}{\hat{s}\hat{t}}$	2.6
$q\bar{q} \to gg$	$\frac{32}{27}\frac{\hat{u}^2+\hat{t}^2}{\hat{u}\hat{t}}-\frac{8}{3}\frac{\hat{u}^2+\hat{t}^2}{\hat{s}^2}$	1.0
$gg \to q\bar{q}$	$\frac{1}{6}\frac{\hat{u}^2+\hat{t}^2}{\hat{u}\hat{t}}-\frac{3}{8}\frac{\hat{u}^2+\hat{t}^2}{\hat{s}^2}$	0.1
$qg \to qg$	$\frac{\hat{s}^2+\hat{u}^2}{\hat{t}^2}-\frac{4}{9}\frac{\hat{s}^2+\hat{u}^2}{\hat{u}\hat{s}}$	6.1
$gg \to gg$	$\frac{9}{4}\left(\frac{\hat{s}^2+\hat{u}^2}{\hat{t}^2}+\frac{\hat{s}^2+\hat{t}^2}{\hat{u}^2}+\frac{\hat{u}^2+\hat{t}^2}{\hat{s}^2}+3\right)$	30.4

Proton-Proton Scattering @ LHC

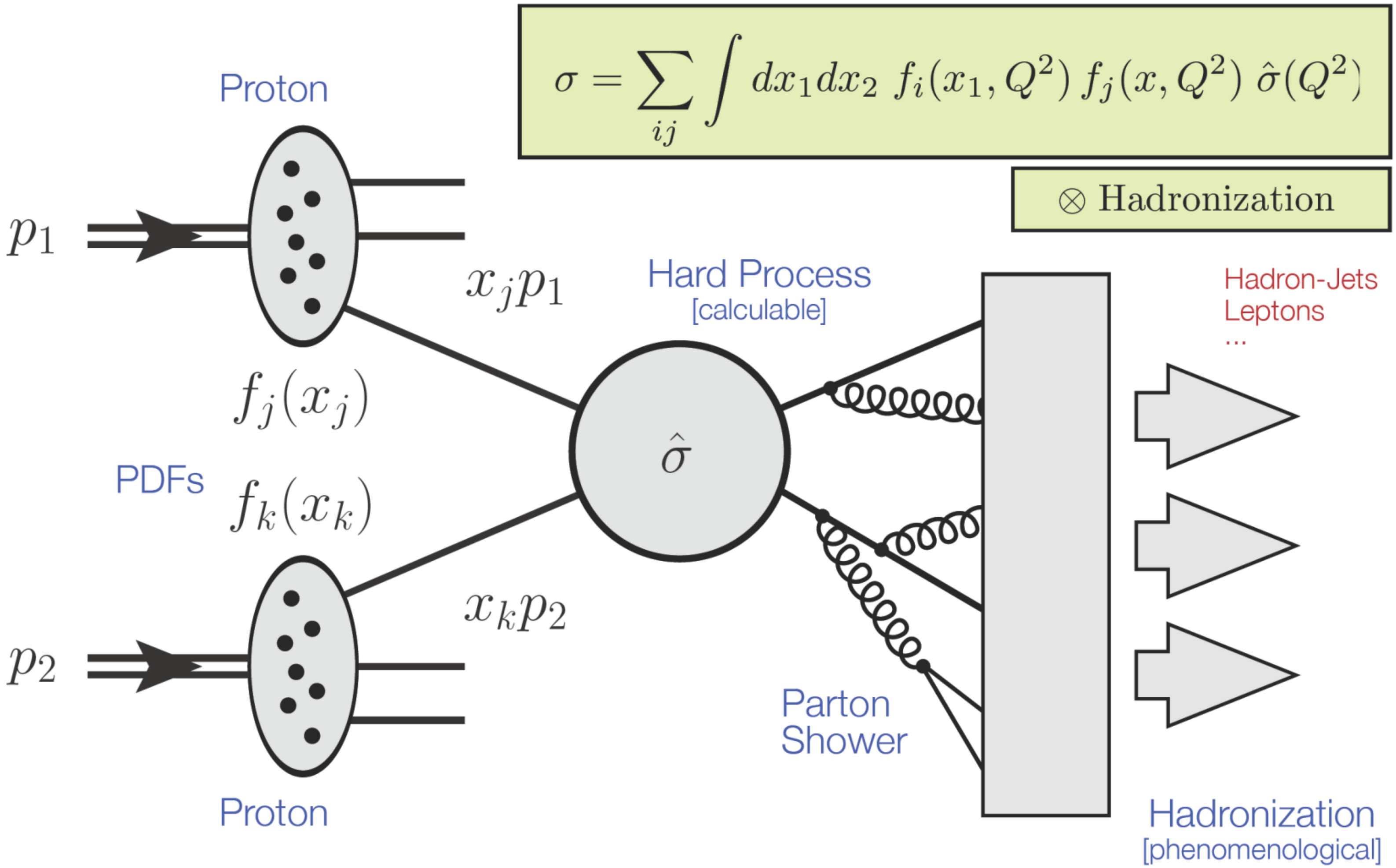

QCD & parton densities

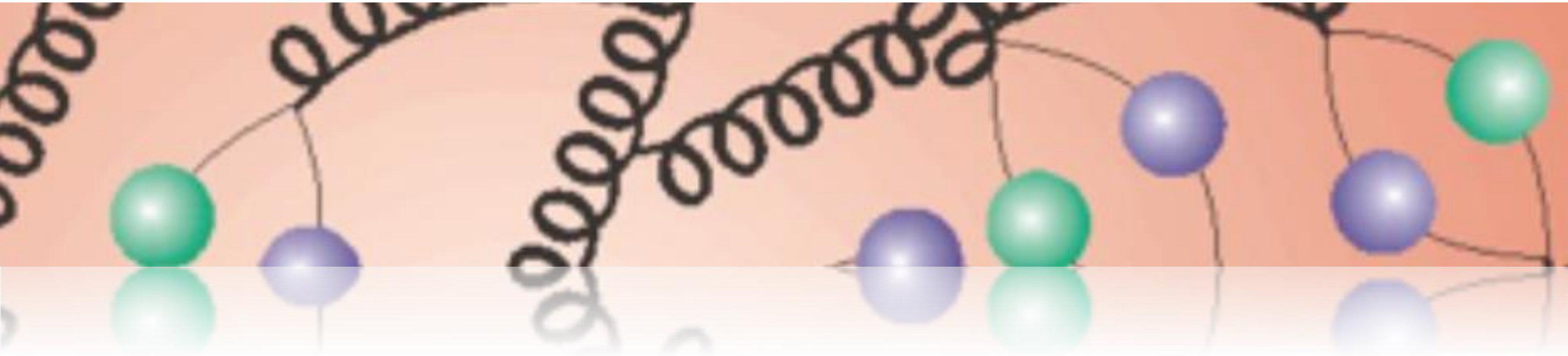

Lepton-proton scattering

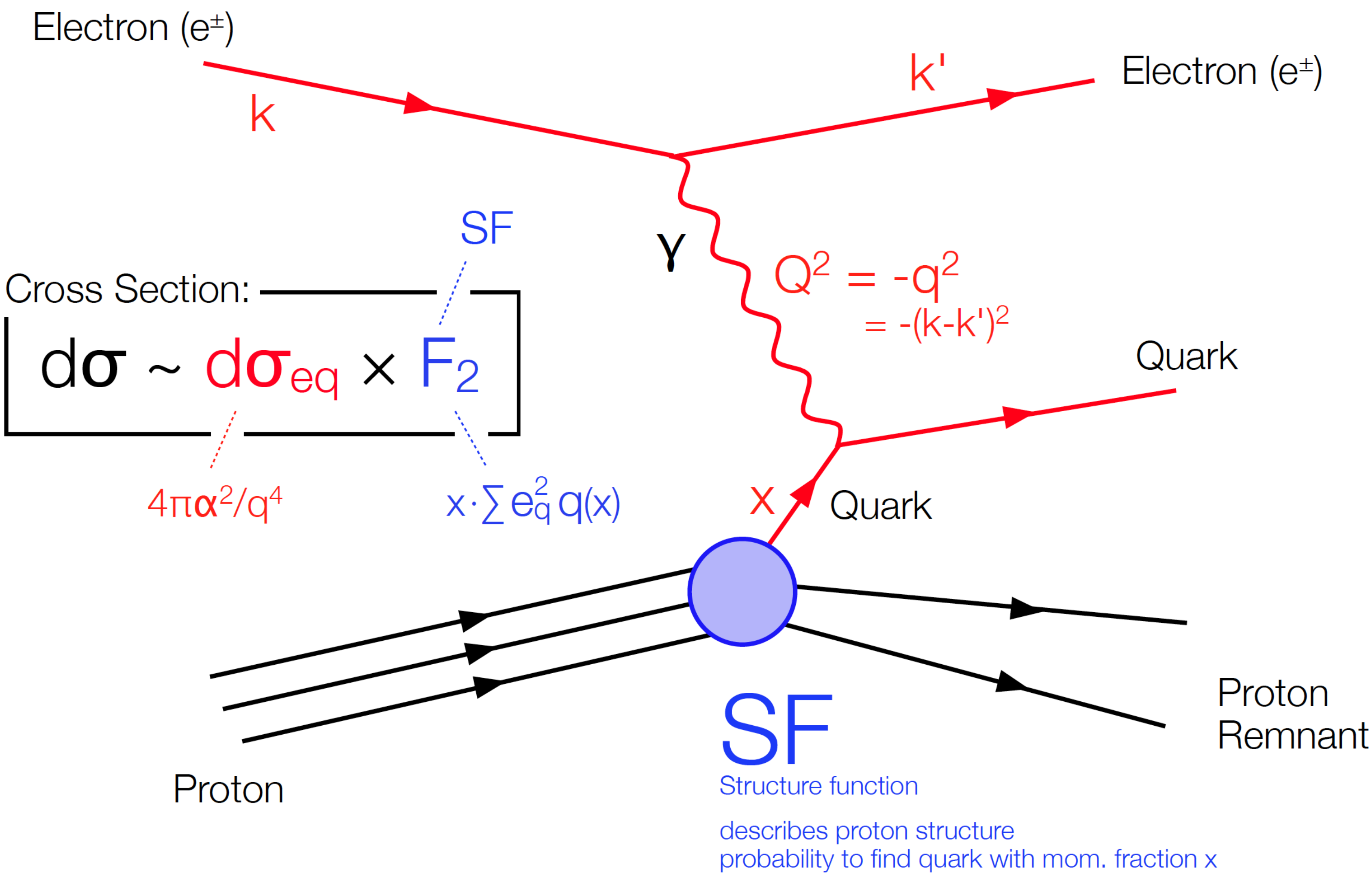

Structure Function F_2

Electron-Quark scattering

(spinless case)

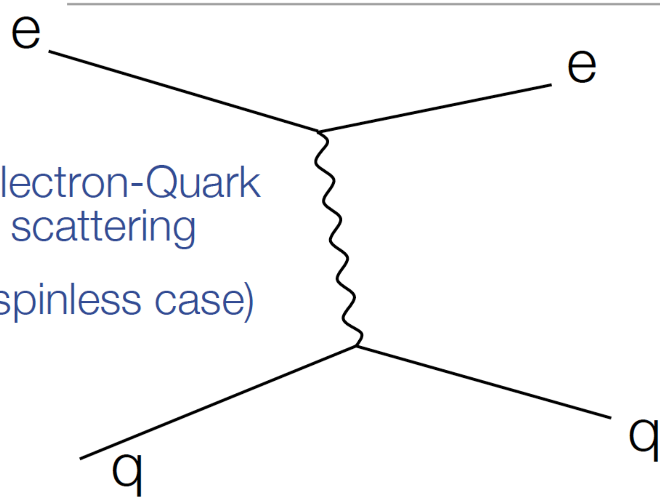

$$\frac{d\sigma(eq)}{dq^2} = \frac{4\pi\alpha^2}{q^4} e_q^2$$

Rutherford scattering on pointlike target

Naive QPM

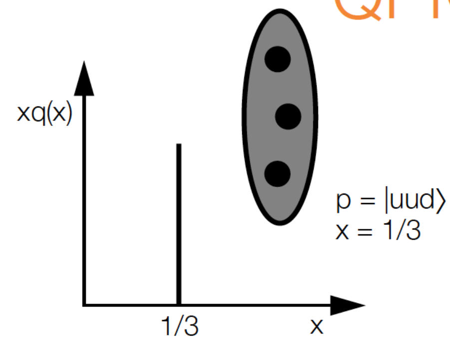

$$\frac{d\sigma(ep)}{dq^2} = \frac{4\pi\alpha^2}{q^4}[2e_u^2 + e_d^2] = \frac{4\pi\alpha^2}{q^4}$$

With quark-quark interactions

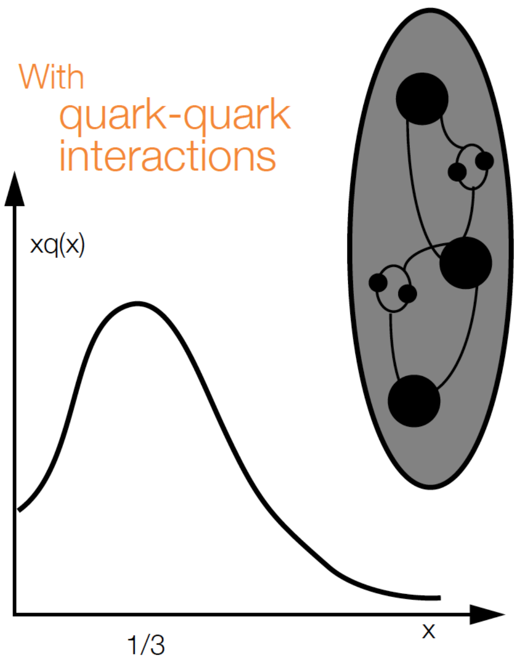

$$\frac{d\sigma(ep)}{dx\, dq^2} = \frac{4\pi\alpha^2}{q^4}[e_u^2 u(x) + e_d^2 d(x) + \ldots]$$

$$= \frac{4\pi\alpha^2}{q^4} \frac{F_2(x)}{x}$$

QPM: Structure Functions F_2 independent of Q^2

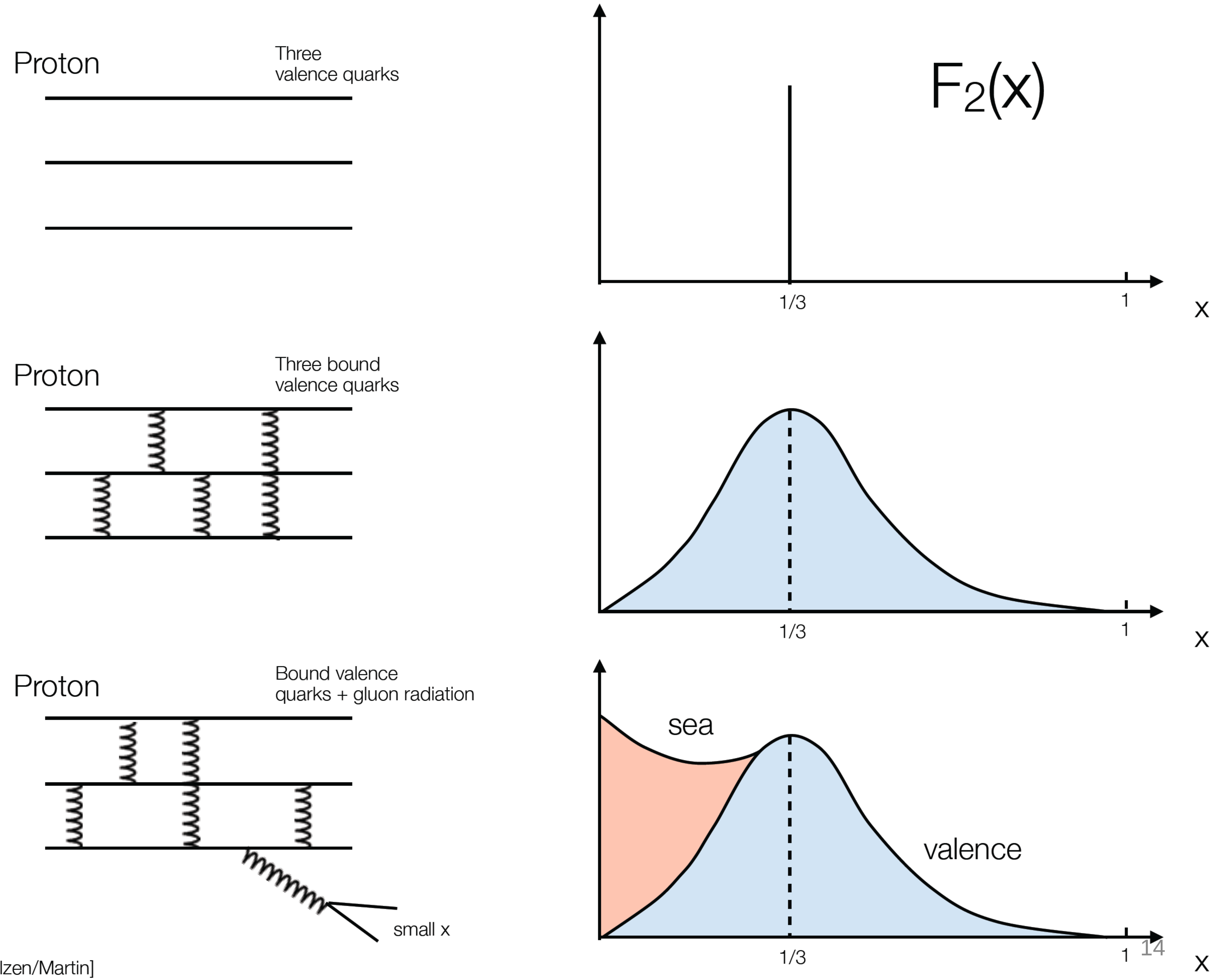

[see e.g. Halzen/Martin]

Scaling violation

$$F_2(x, Q^2) = \sum e_q^2 x q(x, Q^2)$$

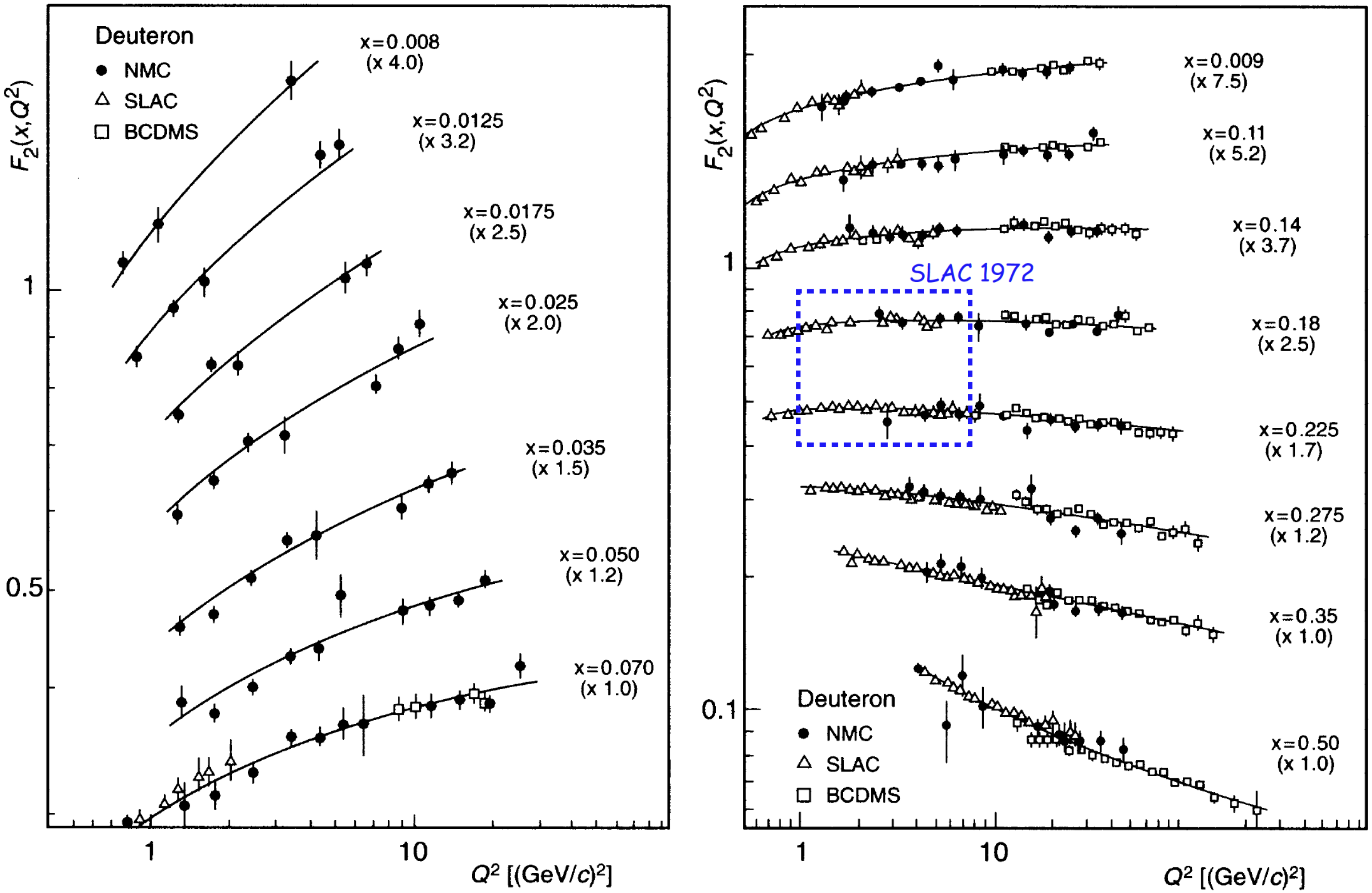

Scaling violation

Proton quark dominated:
$Q^2 \uparrow \Rightarrow F_2 \downarrow$ for fixed x

Proton gluon dominated:
$Q^2 \uparrow \Rightarrow F_2 \uparrow$ for fixed x

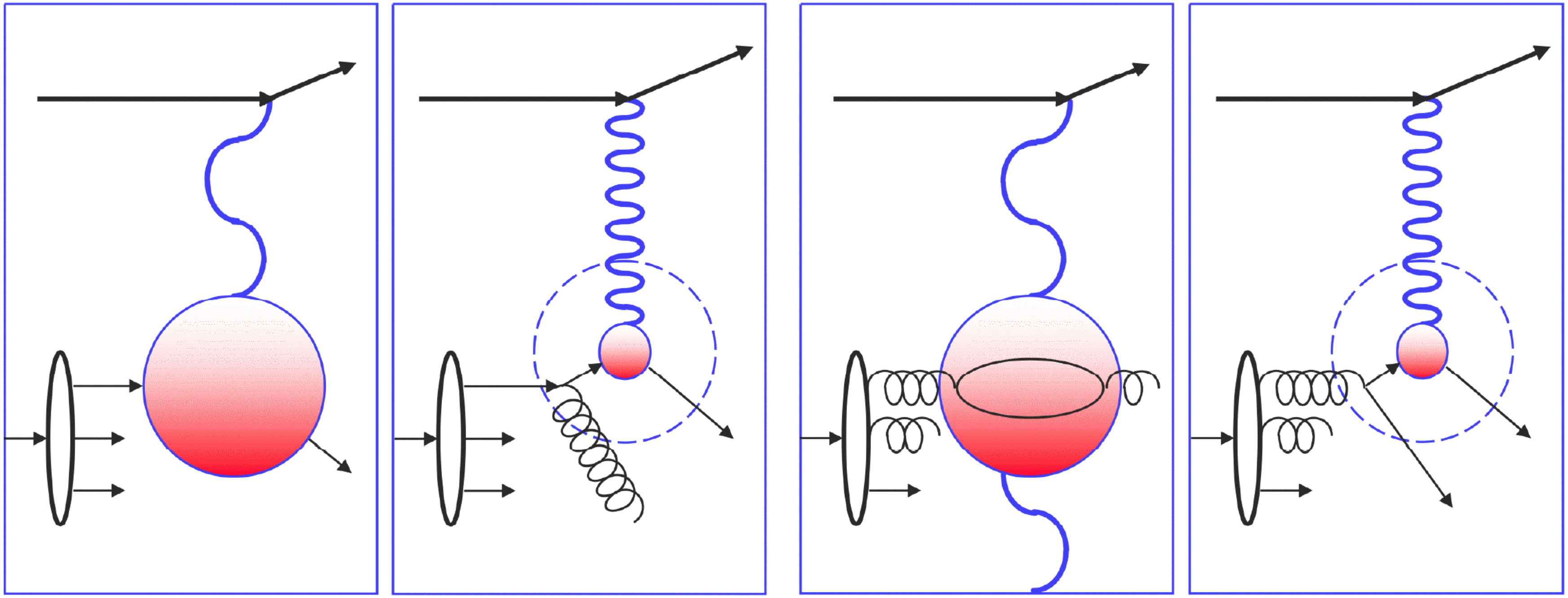

Q^2-evolution described by DGLAP Equations

Proton parton densities

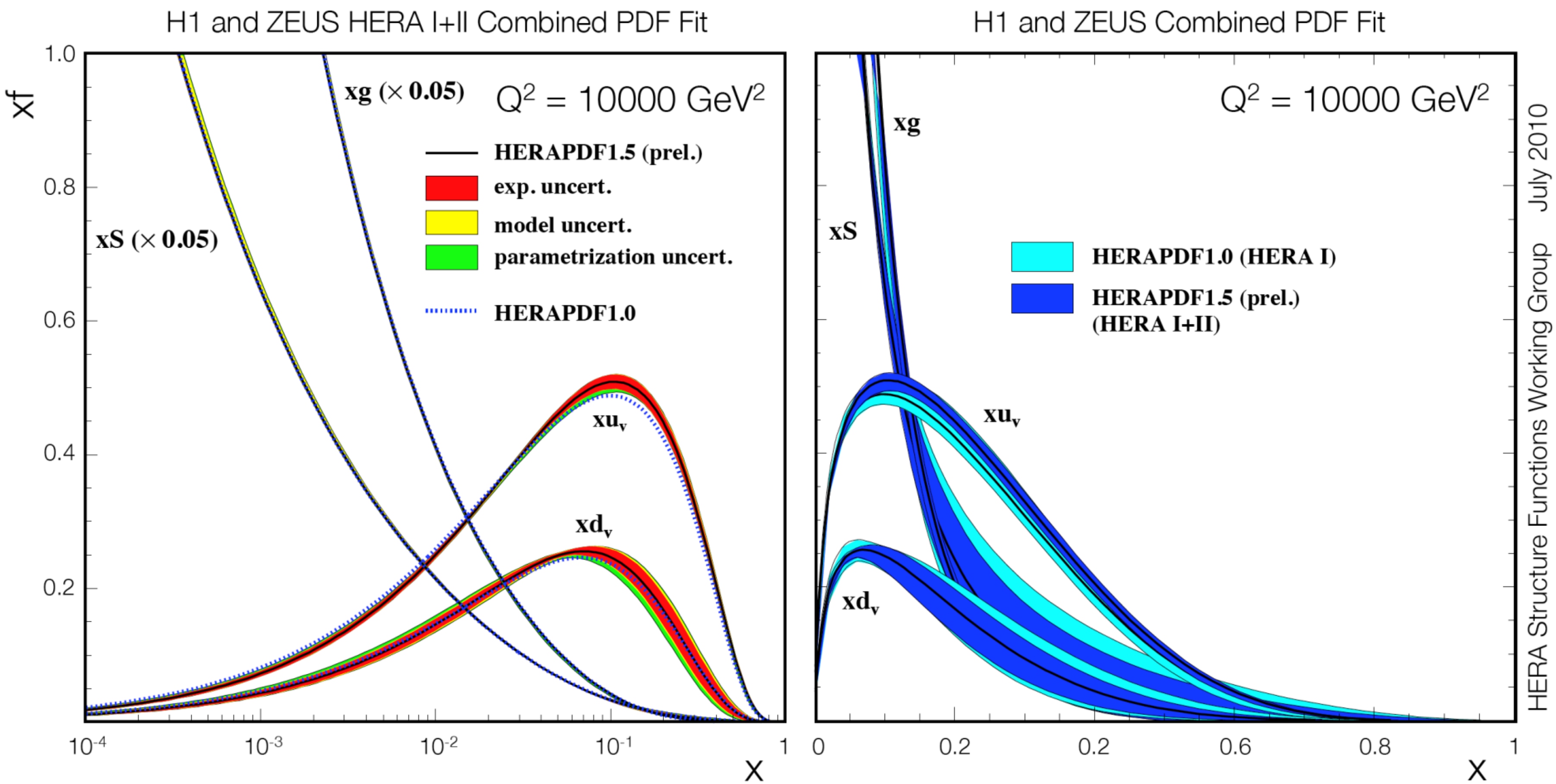

Particle production @ LHC

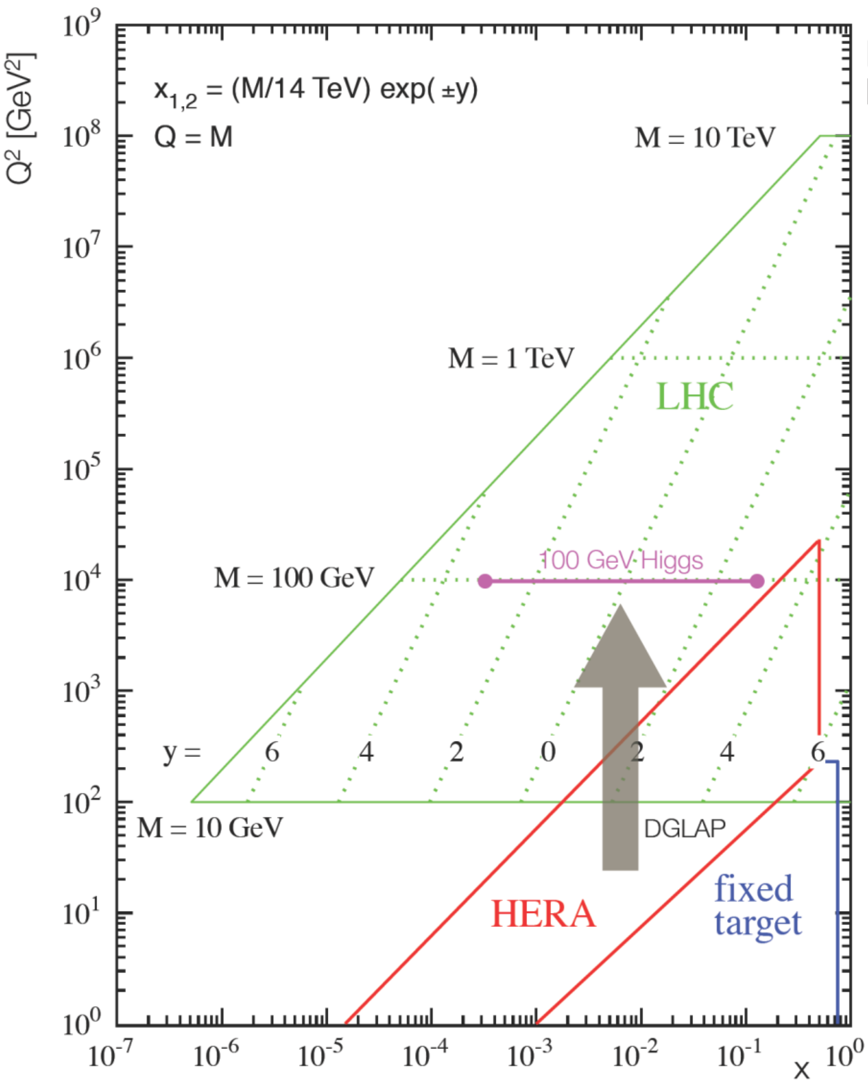

LHC parton kinematics

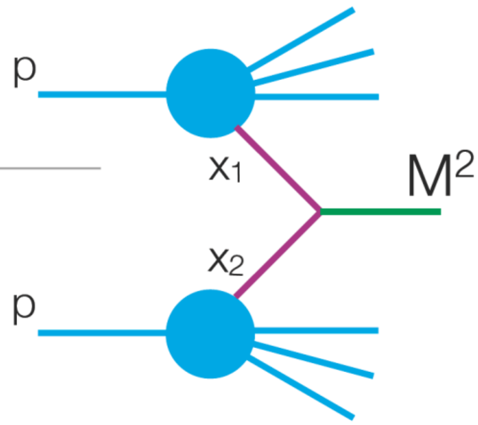

pp ➛ X_M + remnants

X_M: particle with mass M
e.g. Higgs

$$M^2 = x_1 x_2 \cdot s$$

i.e. to produce a particle with mass M at LHC energies ($\sqrt{s}$ = 14 TeV)

$\langle x \rangle = \sqrt{x_1 x_2} = M/\sqrt{s}$
[$x_1 = x_2$: mid-rapidity]

LHC needs:

Knowledge of parton densities
Extrapolation over orders of magnitudes

Monte Carlo Generators

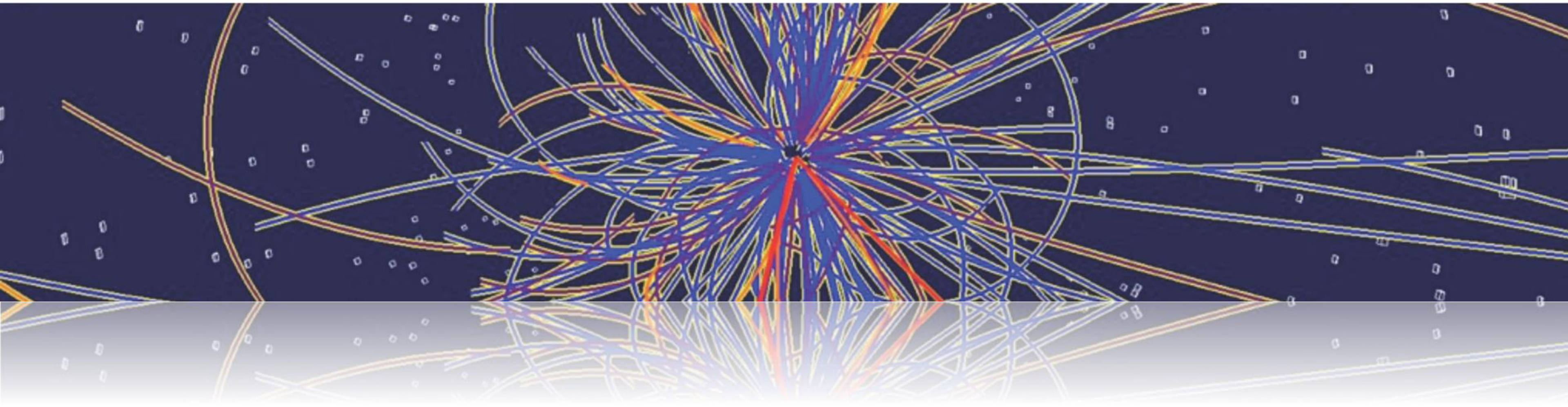

From Partons to Jets

From partons to
color neutral hadrons:

Fragmentation:

Parton splitting into other partons
[QCD: re-summation of leading-logs]
[“Parton shower”]

Hadronization:

Parton shower forms hadrons
[non-perturbative, only models]

Decay of unstable hadrons
[perturbative QCD, electroweak theory]

Fragmentation or
Parton Shower

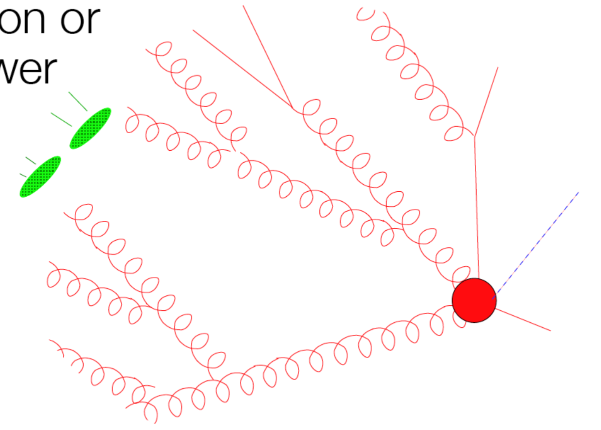

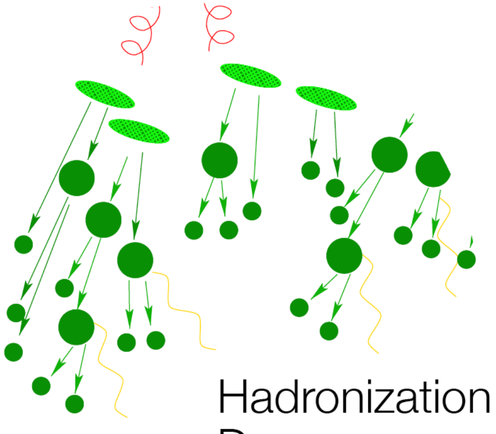

Hadronization &
Decays

Monte Carlo overview

Monte Carlo simulation ...

Numerical process generation
based on random numbers

Method very powerful
in particle physics

Event generation programs:

Pythia, Herwig, Isajet
Sherpa ...

Hard partonic subprocess +
fragmentation & hadronization ...

Detector simulation:

Geant ...

interaction & response
of all produced particles ...

MC simulations in particle physics

Event Generator
simulate physics process
(quantum mechanics: probabilities!)

Detector Simulation
simulate interaction with
detector material

Digitization
translate interactions with
detector into realistic signals

Reconstruction/Analysis
as for real data

Pythia sub-processes

No.	Subprocess
Hard QCD processes:	
11	$f_i f_j \to f_i f_j$
12	$f_i \bar{f}_i \to f_k \bar{f}_k$
13	$f_i \bar{f}_i \to gg$
28	$f_i g \to f_i g$
53	$gg \to f_k \bar{f}_k$
68	$gg \to gg$
Soft QCD processes:	
91	elastic scattering
92	single diffraction (XB)
93	single diffraction (AX)
94	double diffraction
95	low-$p_\perp$ production
Open heavy flavour: (also fourth generation)	
81	$f_i \bar{f}_i \to Q_k \bar{Q}_k$
82	$gg \to Q_k \bar{Q}_k$
83	$q_i f_j \to Q_k f_l$
84	$g\gamma \to Q_k \bar{Q}_k$
85	$\gamma\gamma \to F_k \bar{F}_k$
Closed heavy flavour:	
86	$gg \to J/\psi g$
87	$gg \to \chi_{0c} g$
88	$gg \to \chi_{1c} g$
89	$gg \to \chi_{2c} g$
104	$gg \to \chi_{0c}$
105	$gg \to \chi_{2c}$
106	$gg \to J/\psi\gamma$
107	$g\gamma \to J/\psi g$
108	$\gamma\gamma \to J/\psi\gamma$
W/Z production:	
1	$f_i \bar{f}_i \to \gamma^*/Z^0$
2	$f_i \bar{f}_j \to W^\pm$
22	$f_i \bar{f}_i \to Z^0 Z^0$
23	$f_i \bar{f}_j \to Z^0 W^\pm$
25	$f_i \bar{f}_i \to W^+ W^-$
15	$f_i \bar{f}_i \to g Z^0$
16	$f_i \bar{f}_j \to g W^\pm$
30	$f_i g \to f_i Z^0$
31	$f_i g \to f_k W^\pm$
19	$f_i \bar{f}_i \to \gamma Z^0$
20	$f_i \bar{f}_j \to \gamma W^\pm$
35	$f_i \gamma \to f_i Z^0$

No.	Subprocess
36	$f_i \gamma \to f_k W^\pm$
69	$\gamma\gamma \to W^+ W^-$
70	$\gamma W^\pm \to Z^0 W^\pm$
Prompt photons:	
14	$f_i \bar{f}_i \to g\gamma$
18	$f_i \bar{f}_i \to \gamma\gamma$
29	$f_i g \to f_i \gamma$
114	$gg \to \gamma\gamma$
115	$gg \to g\gamma$
Deeply Inel. Scatt.:	
10	$f_i f_j \to f_k f_l$
99	$\gamma^* q \to q$
Photon-induced:	
33	$f_i \gamma \to f_i g$
34	$f_i \gamma \to f_i \gamma$
54	$g\gamma \to f_k \bar{f}_k$
58	$\gamma\gamma \to f_k \bar{f}_k$
131	$f_i \gamma_T^* \to f_i g$
132	$f_i \gamma_L^* \to f_i g$
133	$f_i \gamma_T^* \to f_i \gamma$
134	$f_i \gamma_L^* \to f_i \gamma$
135	$g\gamma_T^* \to f_i \bar{f}_i$
136	$g\gamma_L^* \to f_i \bar{f}_i$
137	$\gamma_T^* \gamma_T^* \to f_i \bar{f}_i$
138	$\gamma_T^* \gamma_L^* \to f_i \bar{f}_i$
139	$\gamma_L^* \gamma_T^* \to f_i \bar{f}_i$
140	$\gamma_L^* \gamma_L^* \to f_i \bar{f}_i$
80	$q_i \gamma \to q_k \pi^\pm$
Light SM Higgs:	
3	$f_i \bar{f}_i \to h^0$
24	$f_i \bar{f}_i \to Z^0 h^0$
26	$f_i \bar{f}_j \to W^\pm h^0$
32	$f_i g \to f_i h^0$
102	$gg \to h^0$
103	$\gamma\gamma \to h^0$
110	$f_i \bar{f}_i \to \gamma h^0$
111	$f_i \bar{f}_i \to g h^0$
112	$f_i g \to f_i h^0$
113	$gg \to g h^0$
121	$gg \to Q_k \bar{Q}_k h^0$
122	$q_i \bar{q}_i \to Q_k \bar{Q}_k h^0$
123	$f_i f_j \to f_i f_j h^0$
124	$f_i f_j \to f_k f_l h^0$

No.	Subprocess
New gauge bosons:	
141	$f_i \bar{f}_i \to \gamma/Z^0/Z'^0$
142	$f_i \bar{f}_j \to W'^+$
144	$f_i \bar{f}_j \to R$
Heavy SM Higgs:	
5	$Z^0 Z^0 \to h^0$
8	$W^+ W^- \to h^0$
71	$Z_L^0 Z_L^0 \to Z_L^0 Z_L^0$
72	$Z_L^0 Z_L^0 \to W_L^+ W_L^-$
73	$Z_L^0 W_L^\pm \to Z_L^0 W_L^\pm$
76	$W_L^+ W_L^- \to Z_L^0 Z_L^0$
77	$W_L^\pm W_L^\pm \to W_L^\pm W_L^\pm$
BSM Neutral Higgs:	
151	$f_i \bar{f}_i \to H^0$
152	$gg \to H^0$
153	$\gamma\gamma \to H^0$
171	$f_i \bar{f}_i \to Z^0 H^0$
172	$f_i \bar{f}_j \to W^\pm H^0$
173	$f_i f_j \to f_i f_j H^0$
174	$f_i f_j \to f_k f_l H^0$
181	$gg \to Q_k \bar{Q}_k H^0$
182	$q_i \bar{q}_i \to Q_k \bar{Q}_k H^0$
183	$f_i \bar{f}_i \to g H^0$
184	$f_i g \to f_i H^0$
185	$gg \to g H^0$
156	$f_i \bar{f}_i \to A^0$
157	$gg \to A^0$
158	$\gamma\gamma \to A^0$
176	$f_i \bar{f}_i \to Z^0 A^0$
177	$f_i \bar{f}_j \to W^\pm A^0$
178	$f_i f_j \to f_i f_j A^0$
179	$f_i f_j \to f_k f_l A^0$
186	$gg \to Q_k \bar{Q}_k A^0$
187	$q_i \bar{q}_i \to Q_k \bar{Q}_k A^0$
188	$f_i \bar{f}_i \to g A^0$
189	$f_i g \to f_i A^0$
190	$gg \to g A^0$
Charged Higgs:	
143	$f_i \bar{f}_j \to H^+$
161	$f_i g \to f_k H^+$
401	$gg \to \bar{t} b H^+$
402	$q\bar{q} \to \bar{t} b H^+$

No.	Subprocess
Higgs pairs:	
297	$f_i \bar{f}_j \to H^\pm h^0$
298	$f_i \bar{f}_j \to H^\pm H^0$
299	$f_i \bar{f}_i \to A^0 h^0$
300	$f_i \bar{f}_i \to A^0 H^0$
301	$f_i \bar{f}_i \to H^+ H^-$
Leptoquarks:	
145	$q_i \ell_j \to L_Q$
162	$qg \to \ell L_Q$
163	$gg \to L_Q \bar{L}_Q$
164	$q_i \bar{q}_i \to L_Q \bar{L}_Q$
Technicolor:	
149	$gg \to \eta_{tc}$
191	$f_i \bar{f}_i \to \rho_{tc}^0$
192	$f_i \bar{f}_j \to \rho_{tc}^+$
193	$f_i \bar{f}_i \to \omega_{tc}^0$
194	$f_i \bar{f}_i \to f_k \bar{f}_k$
195	$f_i \bar{f}_j \to f_k \bar{f}_l$
361	$f_i \bar{f}_i \to W_L^+ W_L^-$
362	$f_i \bar{f}_i \to W_L^\pm \pi_{tc}^\mp$
363	$f_i \bar{f}_i \to \pi_{tc}^+ \pi_{tc}^-$
364	$f_i \bar{f}_i \to \gamma \pi_{tc}^0$
365	$f_i \bar{f}_i \to \gamma \pi'^0_{tc}$
366	$f_i \bar{f}_i \to Z^0 \pi_{tc}^0$
367	$f_i \bar{f}_i \to Z^0 \pi'^0_{tc}$
368	$f_i \bar{f}_i \to W^\pm \pi_{tc}^\mp$
370	$f_i \bar{f}_j \to W_L^\pm Z_L^0$
371	$f_i \bar{f}_j \to W_L^\pm \pi_{tc}^0$
372	$f_i \bar{f}_j \to \pi_{tc}^\pm Z_L^0$
373	$f_i \bar{f}_j \to \pi_{tc}^\pm \pi_{tc}^0$
374	$f_i \bar{f}_j \to \gamma \pi_{tc}^\pm$
375	$f_i \bar{f}_j \to Z^0 \pi_{tc}^\pm$
376	$f_i \bar{f}_j \to W^\pm \pi_{tc}^0$
377	$f_i \bar{f}_j \to W^\pm \pi'^0_{tc}$
381	$q_i q_j \to q_i q_j$
382	$q_i \bar{q}_i \to q_k \bar{q}_k$
383	$q_i \bar{q}_i \to gg$
384	$f_i g \to f_i g$
385	$gg \to q_k \bar{q}_k$
386	$gg \to gg$
387	$f_i \bar{f}_i \to Q_k \bar{Q}_k$
388	$gg \to Q_k \bar{Q}_k$

No.	Subprocess
Compositeness:	
146	$e\gamma \to e^*$
147	$dg \to d^*$
148	$ug \to u^*$
167	$q_i q_j \to d^* q_k$
168	$q_i q_j \to u^* q_k$
169	$q_i \bar{q}_i \to e^\pm e^{*\mp}$
165	$f_i \bar{f}_i (\to \gamma^*/Z^0) \to f_k \bar{f}_k$
166	$f_i \bar{f}_j (\to W^\pm) \to f_k \bar{f}_l$
Extra Dimensions:	
391	$f\bar{f} \to G^*$
392	$gg \to G^*$
393	$q\bar{q} \to gG^*$
394	$qg \to qG^*$
395	$gg \to gG^*$
Left–right symmetry:	
341	$\ell_i \ell_j \to H_L^{\pm\pm}$
342	$\ell_i \ell_j \to H_R^{\pm\pm}$
343	$\ell_i^\pm \gamma \to H_L^{\pm\pm} e^\mp$
344	$\ell_i^\pm \gamma \to H_R^{\pm\pm} e^\mp$
345	$\ell_i^\pm \gamma \to H_L^{\pm\pm} \mu^\mp$
346	$\ell_i^\pm \gamma \to H_R^{\pm\pm} \mu^\mp$
347	$\ell_i^\pm \gamma \to H_L^{\pm\pm} \tau^\mp$
348	$\ell_i^\pm \gamma \to H_R^{\pm\pm} \tau^\mp$
349	$f_i \bar{f}_i \to H_L^{++} H_L^{--}$
350	$f_i \bar{f}_i \to H_R^{++} H_R^{--}$
351	$f_i f_j \to f_k f_l H_L^{\pm\pm}$
352	$f_i f_j \to f_k f_l H_R^{\pm\pm}$
353	$f_i \bar{f}_i \to Z_R^0$
354	$f_i \bar{f}_j \to W_R^\pm$
SUSY:	
201	$f_i \bar{f}_i \to \tilde{e}_L \tilde{e}_L^*$
202	$f_i \bar{f}_i \to \tilde{e}_R \tilde{e}_R^*$
203	$f_i \bar{f}_i \to \tilde{e}_L \tilde{e}_R^* +$
204	$f_i \bar{f}_i \to \tilde{\mu}_L \tilde{\mu}_L^*$
205	$f_i \bar{f}_i \to \tilde{\mu}_R \tilde{\mu}_R^*$
206	$f_i \bar{f}_i \to \tilde{\mu}_L \tilde{\mu}_R^* +$
207	$f_i \bar{f}_i \to \tilde{\tau}_1 \tilde{\tau}_1^*$
208	$f_i \bar{f}_i \to \tilde{\tau}_2 \tilde{\tau}_2^*$
209	$f_i \bar{f}_i \to \tilde{\tau}_1 \tilde{\tau}_2^* +$

No.	Subprocess
210	$f_i \bar{f}_j \to \tilde{\ell}_L \tilde{\nu}_\ell^* +$
211	$f_i \bar{f}_j \to \tilde{\tau}_1 \tilde{\nu}_\tau^* +$
212	$f_i \bar{f}_j \to \tilde{\tau}_2 \tilde{\nu}_\tau^* +$
213	$f_i \bar{f}_i \to \tilde{\nu}_\ell \tilde{\nu}_\ell{}^*$
214	$f_i \bar{f}_i \to \tilde{\nu}_\tau \tilde{\nu}_\tau^*$
216	$f_i \bar{f}_i \to \tilde{\chi}_1 \tilde{\chi}_1$
217	$f_i \bar{f}_i \to \tilde{\chi}_2 \tilde{\chi}_2$
218	$f_i \bar{f}_i \to \tilde{\chi}_3 \tilde{\chi}_3$
219	$f_i \bar{f}_i \to \tilde{\chi}_4 \tilde{\chi}_4$
220	$f_i \bar{f}_i \to \tilde{\chi}_1 \tilde{\chi}_2$
221	$f_i \bar{f}_i \to \tilde{\chi}_1 \tilde{\chi}_3$
222	$f_i \bar{f}_i \to \tilde{\chi}_1 \tilde{\chi}_4$
223	$f_i \bar{f}_i \to \tilde{\chi}_2 \tilde{\chi}_3$
224	$f_i \bar{f}_i \to \tilde{\chi}_2 \tilde{\chi}_4$
225	$f_i \bar{f}_i \to \tilde{\chi}_3 \tilde{\chi}_4$
226	$f_i \bar{f}_i \to \tilde{\chi}_1^\pm \tilde{\chi}_1^\mp$
227	$f_i \bar{f}_i \to \tilde{\chi}_2^\pm \tilde{\chi}_2^\mp$
228	$f_i \bar{f}_i \to \tilde{\chi}_1^\pm \tilde{\chi}_2^\mp$
229	$f_i \bar{f}_j \to \tilde{\chi}_1 \tilde{\chi}_1^\pm$
230	$f_i \bar{f}_j \to \tilde{\chi}_2 \tilde{\chi}_1^\pm$
231	$f_i \bar{f}_j \to \tilde{\chi}_3 \tilde{\chi}_1^\pm$
232	$f_i \bar{f}_j \to \tilde{\chi}_4 \tilde{\chi}_1^\pm$
233	$f_i \bar{f}_j \to \tilde{\chi}_1 \tilde{\chi}_2^\pm$
234	$f_i \bar{f}_j \to \tilde{\chi}_2 \tilde{\chi}_2^\pm$
235	$f_i \bar{f}_j \to \tilde{\chi}_3 \tilde{\chi}_2^\pm$
236	$f_i \bar{f}_j \to \tilde{\chi}_4 \tilde{\chi}_2^\pm$
237	$f_i \bar{f}_i \to \tilde{g} \tilde{\chi}_1$
238	$f_i \bar{f}_i \to \tilde{g} \tilde{\chi}_2$
239	$f_i \bar{f}_i \to \tilde{g} \tilde{\chi}_3$
240	$f_i \bar{f}_i \to \tilde{g} \tilde{\chi}_4$
241	$f_i \bar{f}_j \to \tilde{g} \tilde{\chi}_1^\pm$
242	$f_i \bar{f}_j \to \tilde{g} \tilde{\chi}_2^\pm$
243	$f_i \bar{f}_i \to \tilde{g} \tilde{g}$
244	$gg \to \tilde{g} \tilde{g}$
246	$f_i g \to \tilde{q}_{iL} \tilde{\chi}_1$
247	$f_i g \to \tilde{q}_{iR} \tilde{\chi}_1$
248	$f_i g \to \tilde{q}_{iL} \tilde{\chi}_2$
249	$f_i g \to \tilde{q}_{iR} \tilde{\chi}_2$

No.	Subprocess
250	$f_i g \to \tilde{q}_{iL} \tilde{\chi}_3$
251	$f_i g \to \tilde{q}_{iR} \tilde{\chi}_3$
252	$f_i g \to \tilde{q}_{iL} \tilde{\chi}_4$
253	$f_i g \to \tilde{q}_{iR} \tilde{\chi}_4$
254	$f_i g \to \tilde{q}_{jL} \tilde{\chi}_1^\pm$
256	$f_i g \to \tilde{q}_{jL} \tilde{\chi}_2^\pm$
258	$f_i g \to \tilde{q}_{iL} \tilde{g}$
259	$f_i g \to \tilde{q}_{iR} \tilde{g}$
261	$f_i \bar{f}_i \to \tilde{t}_1 \tilde{t}_1^*$
262	$f_i \bar{f}_i \to \tilde{t}_2 \tilde{t}_2^*$
263	$f_i \bar{f}_i \to \tilde{t}_1 \tilde{t}_2^* +$
264	$gg \to \tilde{t}_1 \tilde{t}_1^*$
265	$gg \to \tilde{t}_2 \tilde{t}_2^*$
271	$f_i f_j \to \tilde{q}_{iL} \tilde{q}_{jL}$
272	$f_i f_j \to \tilde{q}_{iR} \tilde{q}_{jR}$
273	$f_i f_j \to \tilde{q}_{iL} \tilde{q}_{jR} +$
274	$f_i \bar{f}_j \to \tilde{q}_{iL} \tilde{q}_{jL}^*$
275	$f_i \bar{f}_j \to \tilde{q}_{iR} \tilde{q}_{jR}^*$
276	$f_i \bar{f}_j \to \tilde{q}_{iL} \tilde{q}_{jR}^* +$
277	$f_i \bar{f}_i \to \tilde{q}_{jL} \tilde{q}_{jL}^*$
278	$f_i \bar{f}_i \to \tilde{q}_{jR} \tilde{q}_{jR}^*$
279	$gg \to \tilde{q}_{iL} \tilde{q}_{iL}^*$
280	$gg \to \tilde{q}_{iR} \tilde{q}_{iR}^*$
281	$bq_i \to \tilde{b}_1 \tilde{q}_{iL}$
282	$bq_i \to \tilde{b}_2 \tilde{q}_{iR}$
283	$bq_i \to \tilde{b}_1 \tilde{q}_{iR} +$
284	$b\bar{q}_i \to \tilde{b}_1 \tilde{q}_{iL}^*$
285	$b\bar{q}_i \to \tilde{b}_2 \tilde{q}_{iR}^*$
286	$b\bar{q}_i \to \tilde{b}_1 \tilde{q}_{iR}^* +$
287	$f_i \bar{f}_i \to \tilde{b}_1 \tilde{b}_1^*$
288	$f_i \bar{f}_i \to \tilde{b}_2 \tilde{b}_2^*$
289	$gg \to \tilde{b}_1 \tilde{b}_1^*$
290	$gg \to \tilde{b}_2 \tilde{b}_2^*$
291	$bb \to \tilde{b}_1 \tilde{b}_1$
292	$bb \to \tilde{b}_2 \tilde{b}_2$
293	$bb \to \tilde{b}_1 \tilde{b}_2$
294	$bg \to \tilde{b}_1 \tilde{g}$
295	$bg \to \tilde{b}_2 \tilde{g}$
296	$b\bar{b} \to \tilde{b}_1 \tilde{b}_2^* +$

Detector simulation

GEANT
Geometry And Tracking

Detailed description of detector geometry
[sensitive & insensitive volumes]

Tracking of all particles through detector material ...

➛ Detector response

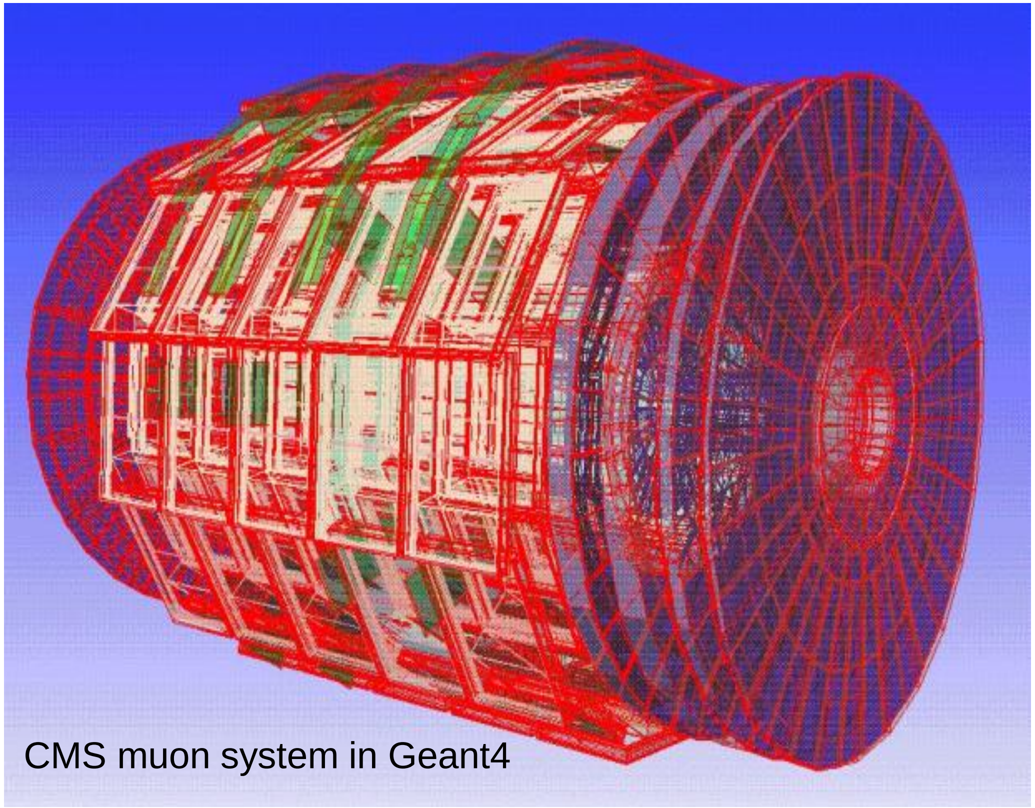

CMS muon system in Geant4

Developed at CERN since 1974 (FORTRAN)
[Today: Geant4; programmed in C^{++}]

Luminosity
and cross-section measurements

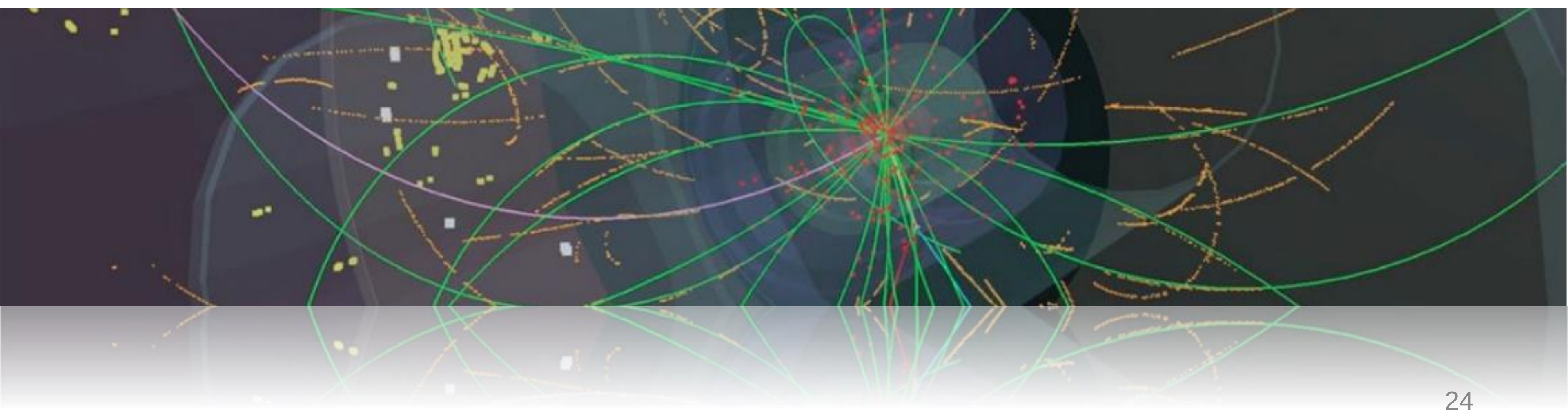

Cross section & Luminosity

Number of observed events

just count …

Background

measured from data or calculated from theory

$$\sigma = \frac{N^{\mathrm{obs}} - N^{\mathrm{bkg}}}{\int \mathcal{L}\, \mathrm{d}t \cdot \varepsilon}$$

Luminosity

determined by accelerator, triggers, …

Efficiency

many factors, optimized by experimentalist

Cross section & Luminosity

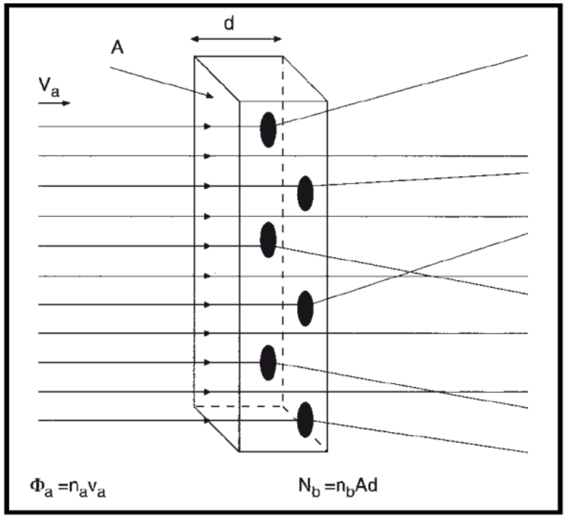

$$\Phi_a = \frac{\dot{N}_a}{A} = n_a v_a$$

Φ_a : flux
n_a : density of particle beam
v_a : velocity of beam particles

$$\dot{N} = \Phi_a \cdot N_b \cdot \sigma_b$$

$\dot{N}$: reaction rate
N_b : target particles within beam area
σ_a : effective area of single scattering center

$$L = \Phi_a \cdot N_b$$

L : luminosity

$$\dot{N} \equiv L \cdot \sigma$$

$$N = \sigma \cdot \underbrace{\int L\,dt}_{\text{integrated luminosity}} \qquad \sigma = N/L$$

Collider experiment:

$$\Phi_a = \frac{\dot{N}_a}{A} = \frac{N_a \cdot n \cdot v/U}{A} = \frac{N_a \cdot n \cdot f}{A}$$

$$L = f\frac{nN_aN_b}{A} = f\frac{nN_aN_b}{4\pi\sigma_x\sigma_y}$$

LHC:

N_x	~	10^{11}
A	~	.0005 mm^2
n	~	2800
f	~	11 kHz
L	~	10^{34} cm^{-2} s^{-1}

N_a : number of particles per bunch (beam A)
N_b : number of particles per bunch (beam B)
U : circumference of ring
n : number of bunches per beam
v : velocity of beam particles
f : revolution frequency
A : beam cross-section
σ_x : standard deviation of beam profile in x
σ_y : standard deviation of beam profile in y

Van-der-Meer separation scan

Determine beam size ...

measuring size and shape of the interaction region by recording relative interaction rates as a function of transverse beam separation ...

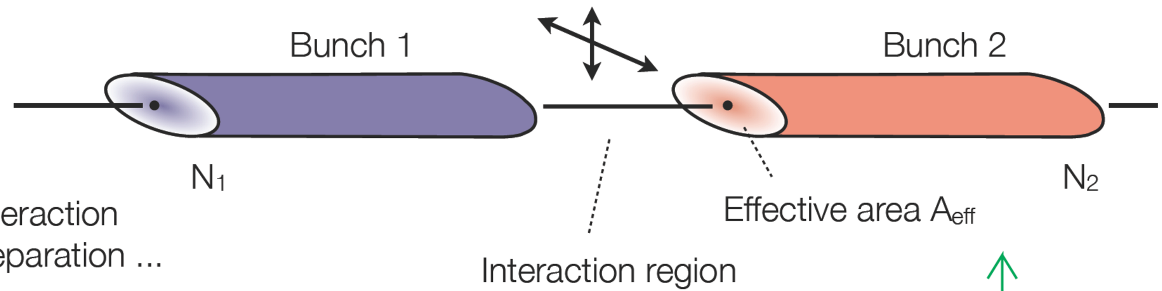

[LHC Project Report 1019: H. Burkhardt et al.]

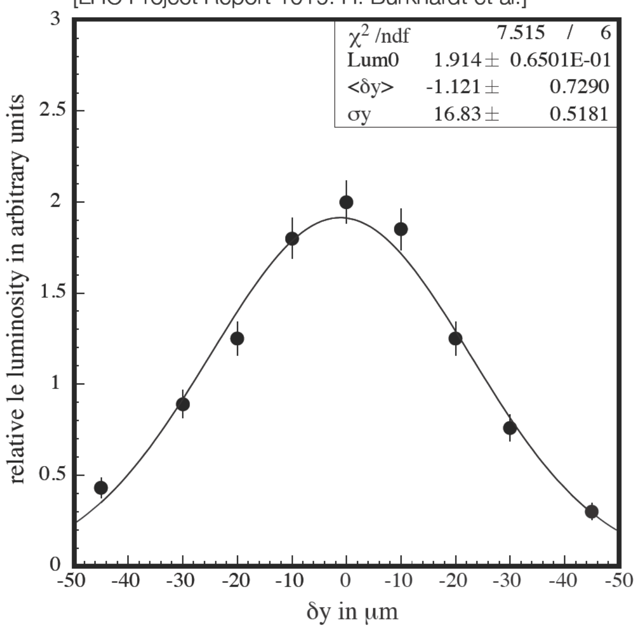

$$\frac{L}{L_0} = \exp\left[- \left(\frac{\delta_x}{2\sigma_x} \right)^2 - \left(\frac{\delta_y}{2\sigma_y} \right)^2 \right]$$

[IPAC 2010, S. White et al.]

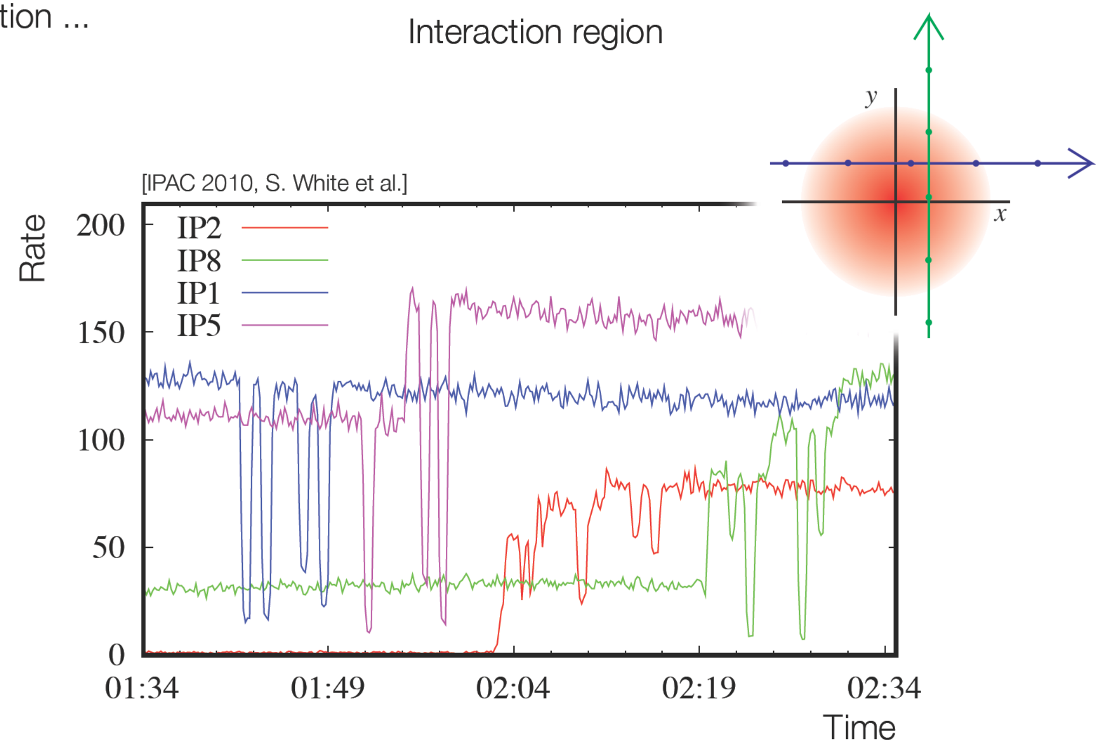

First optimization scans at LHC performed for squeezed optics in all IPs [November 2009].

Minimum bias events

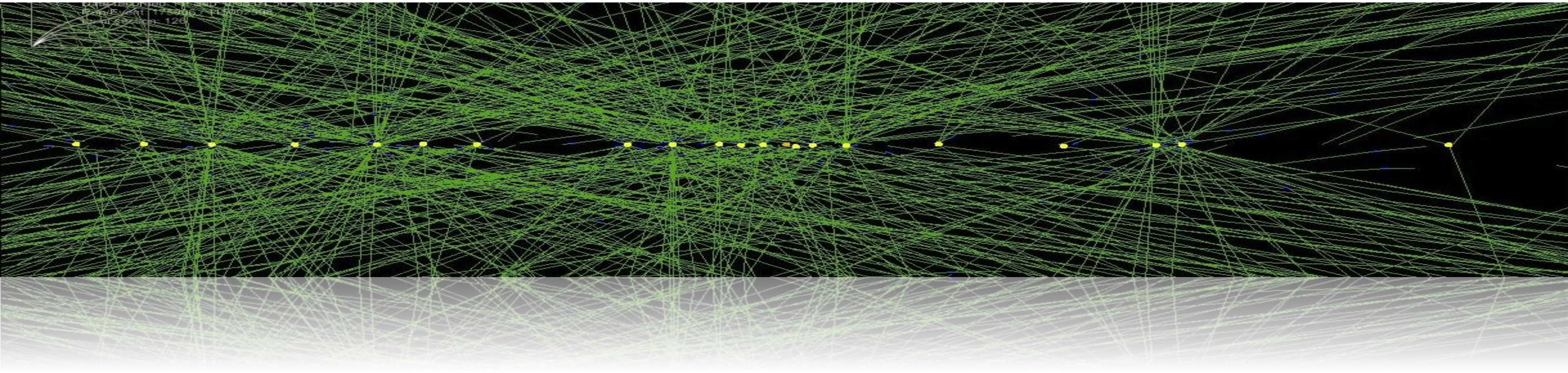

Characteristics of inelastic p-p collisions

Particle density in minimum bias events

Soft QCD (PT threshold on tracks: 50 MeV)

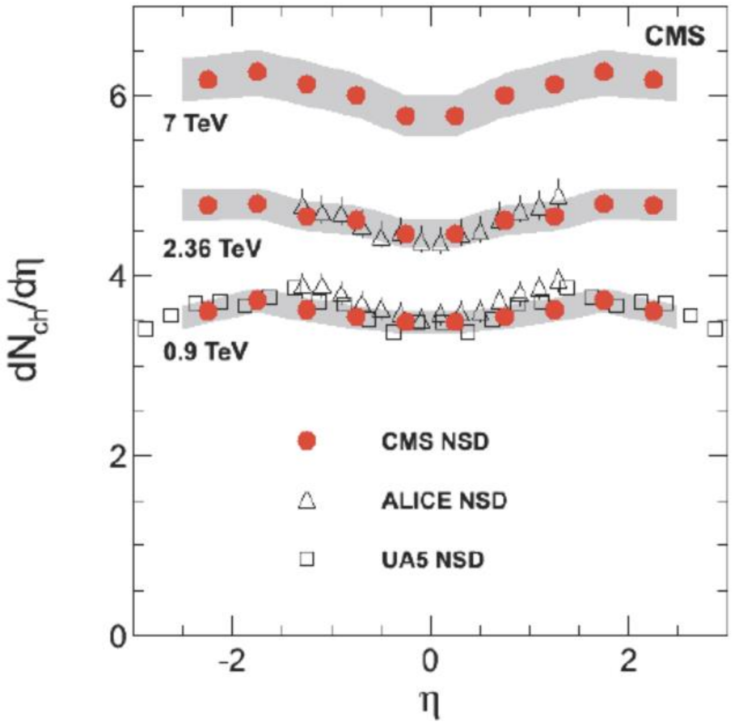

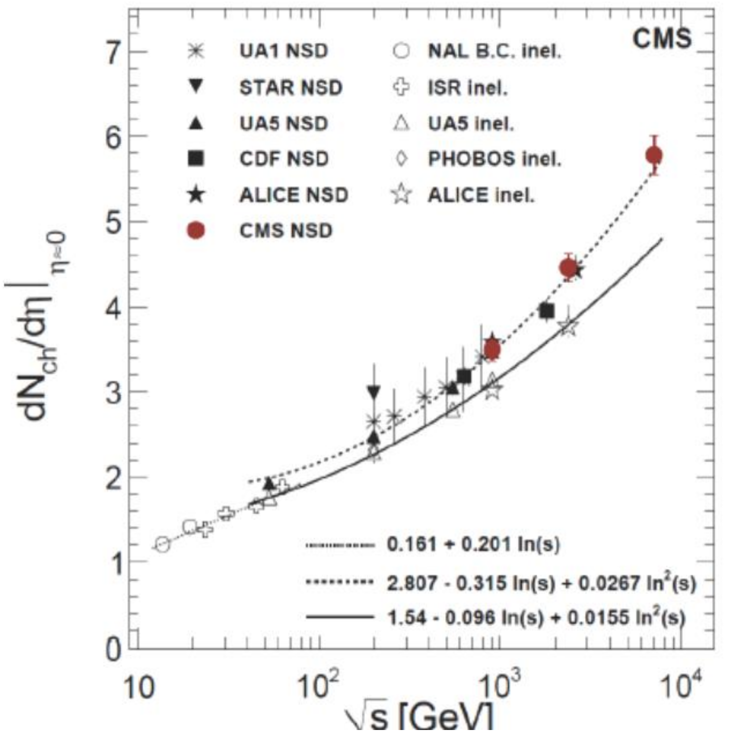

Particle density in data rises faster than in model predictions.
Tuning of MC generators was needed.

Charged particle p_T spectrum

$<p_T> = 0.545$
$\pm$ 0.005 (stat.)
$\pm$ 0.015 (syst.) GeV/c

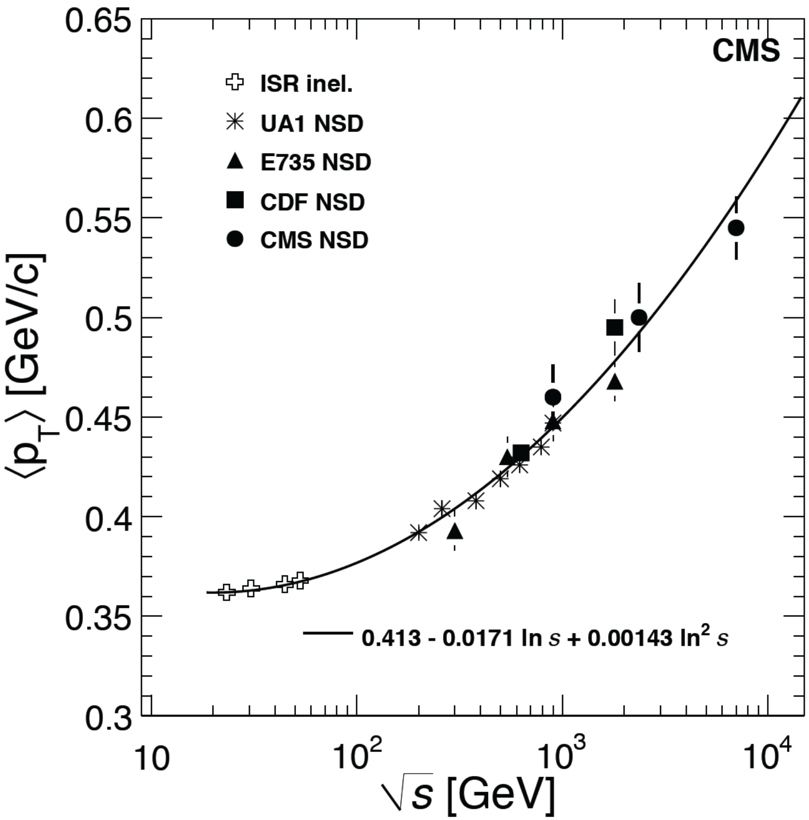

dN_{ch}/dp_T

p_T > 100 MeV
$|\eta|$ < 2.5
$N_{ch} \geq 2$

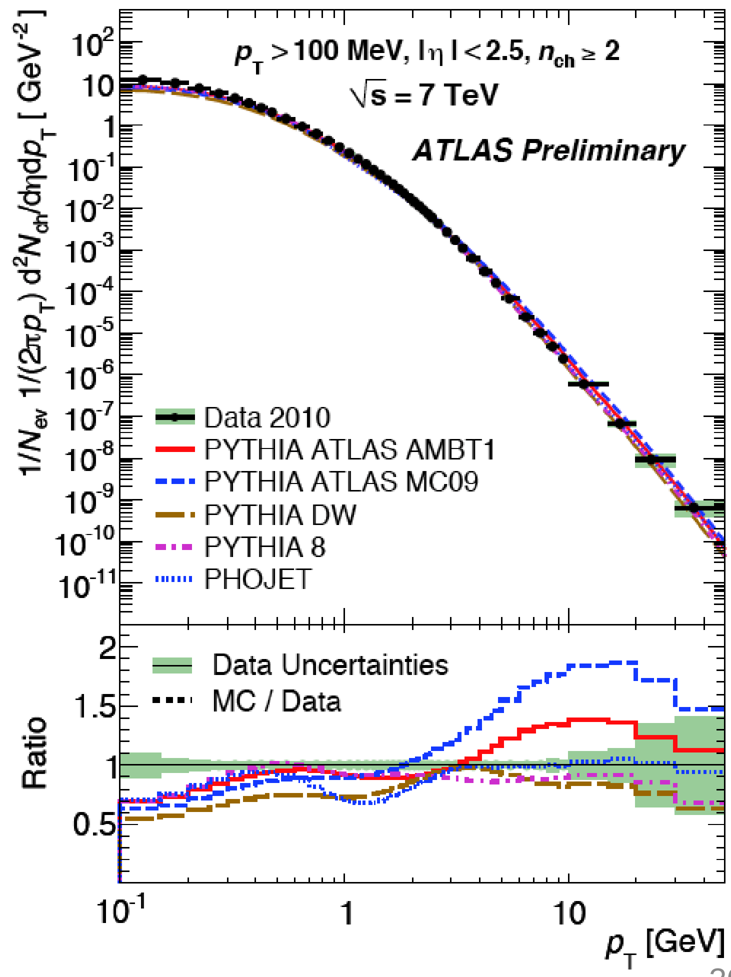

Jet physics

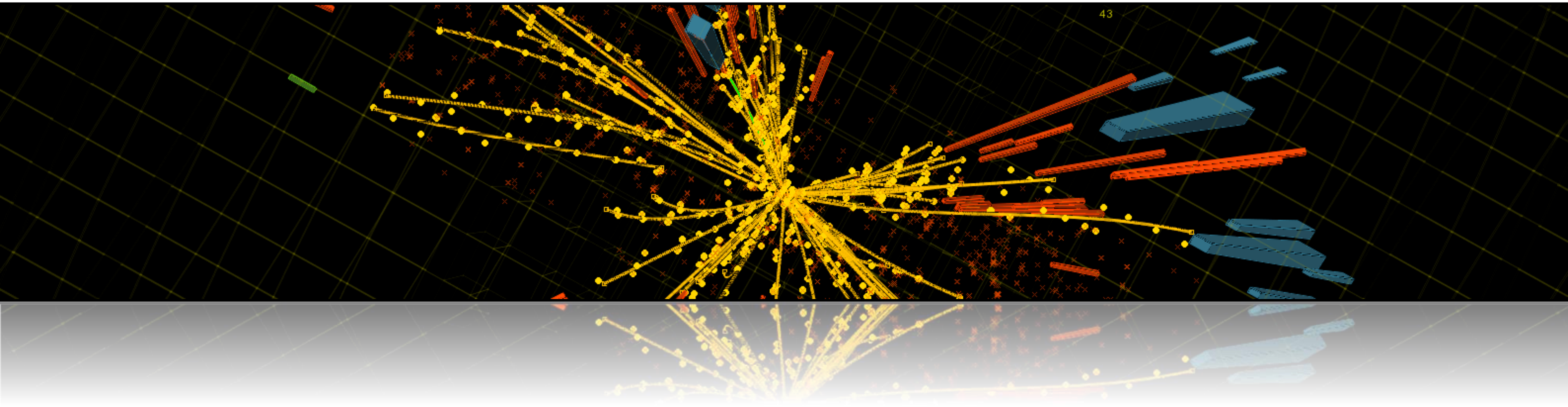

Jet production @ LHC

$$\sigma = \sum_{ij} \int dx_1 dx_2 \; f_i(x_1, Q^2) \; f_j(x, Q^2) \; \hat{\sigma}(Q^2)$$

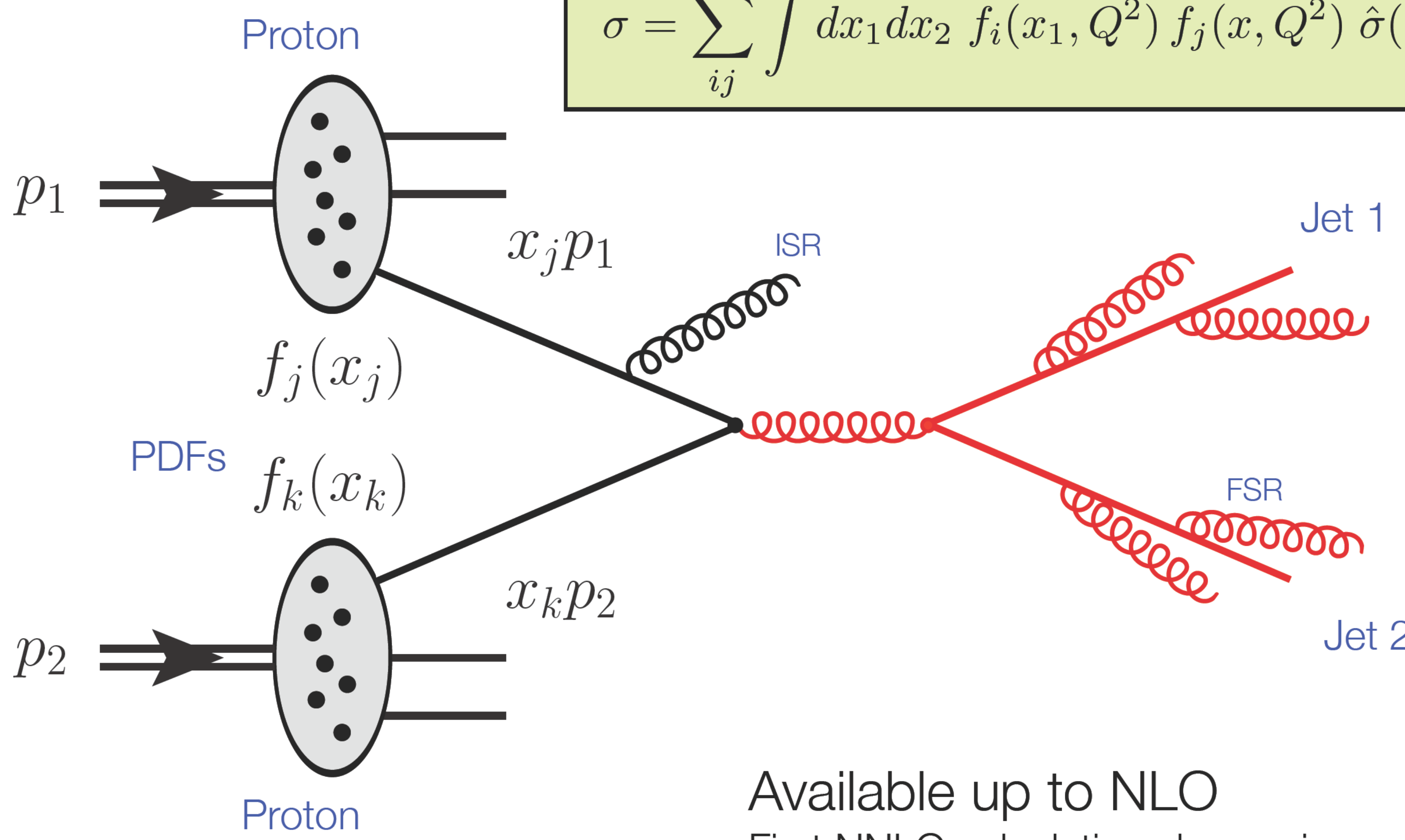

Available up to NLO

First NNLO calculations becoming available ...

Scale uncertainty

$$\sigma = \sum_{ij} \int dx_1 dx_2\ f_i(x_1, \mu_F^2)\ f_j(x, \mu_F^2)\ \hat{\sigma}(\mu_R^2)$$

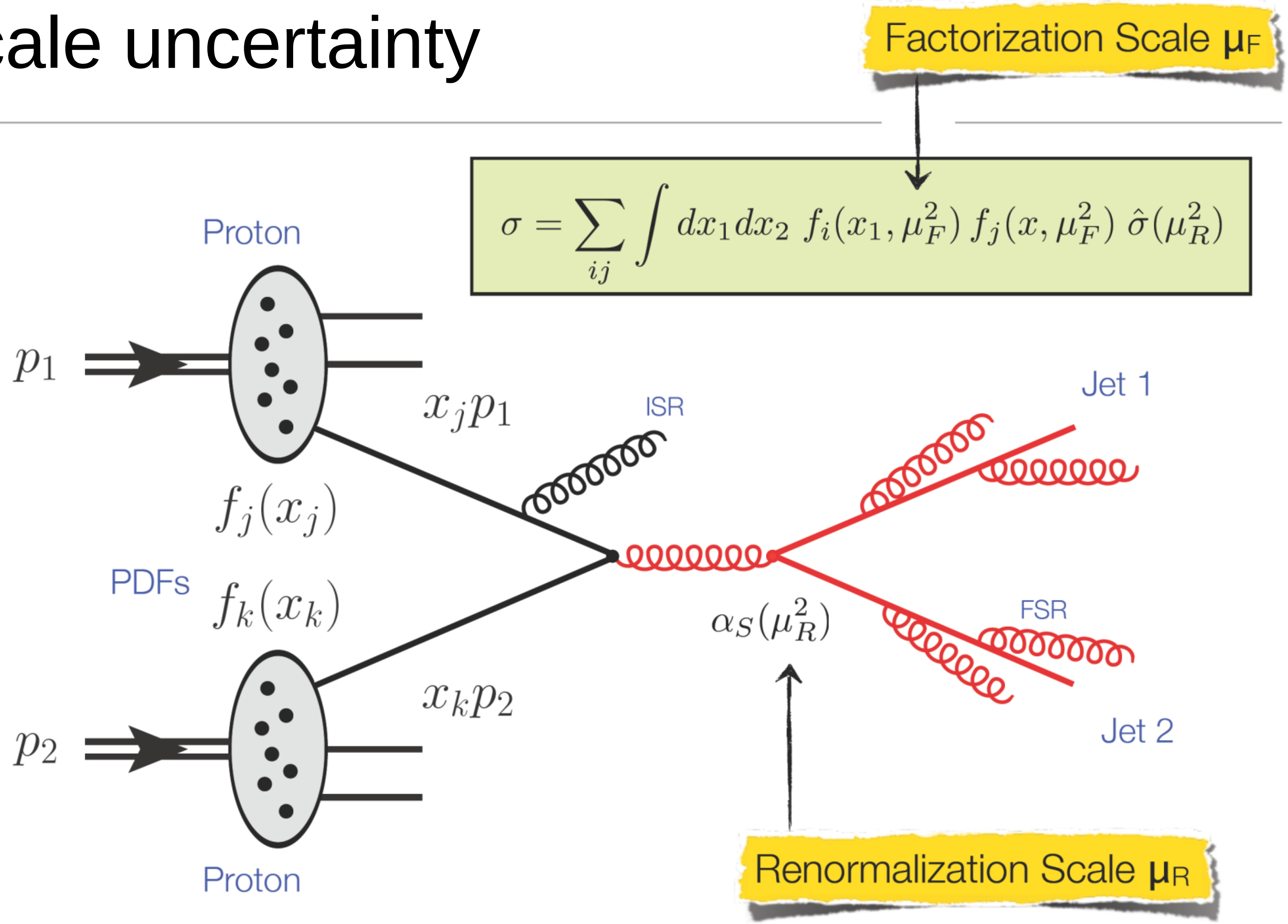

The default renormalization and factorization scales (μ_R and μ_F respectively) are defined to be equal to the p_T of the leading jet in the event

Scale uncertainty estimation: vary μ_R, μ_F within [$\mu_R/2$, $2\mu_R$] and [$\mu_F/2$, $2\mu_F$]

Jet properties measurement

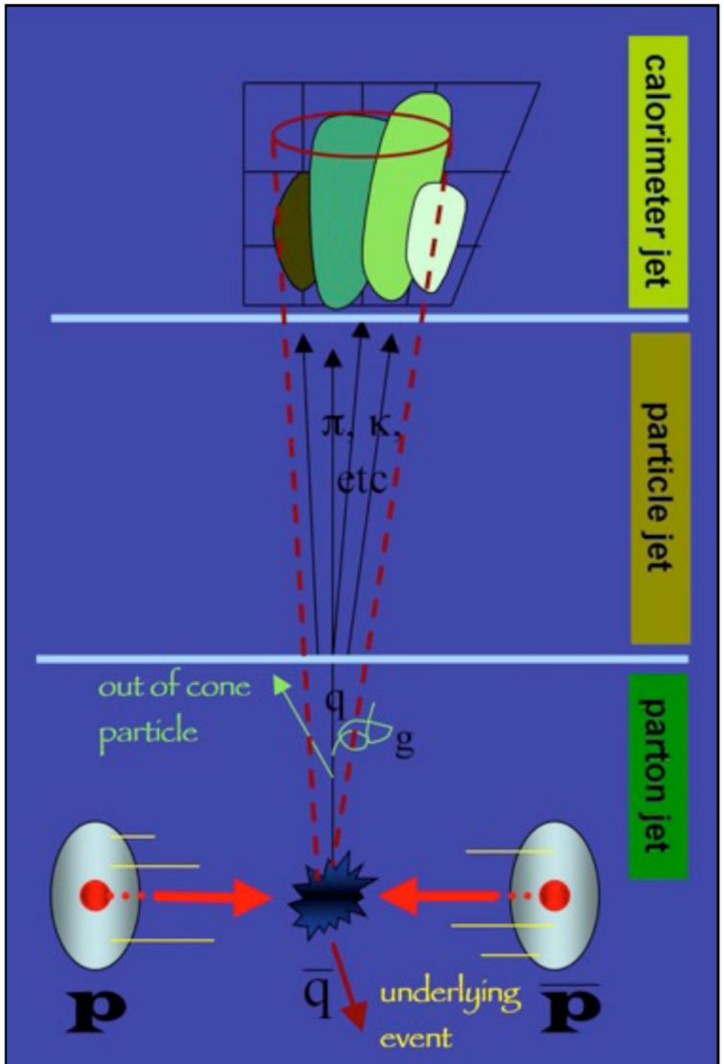

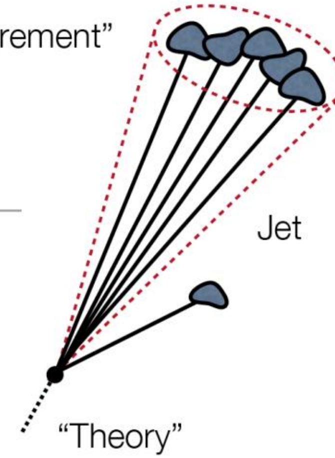

Calorimeter Jet
[extracted from calorimeter clusters]

Understanding of detector response
Knowledge about dead material
Correct signal calibration
Potentially include tracks

From measured energy to particle energy

Compensate energy loss due to neutrinos, nuclear excitation ...

Hadron Jet
[might include electrons, muons ...]

Hadronization
Fragmentation
Parton shower
Particle decays

From particle energy to original parton energy

Compensate hadronization; energy in/outside jet cone ...

Parton Jet
[quarks and gluons]

Proton-proton interactions
Initial and final state radiation
Underlying event

Needs Calibration

Jet reconstruction

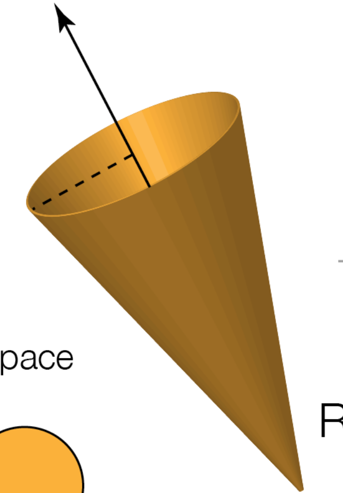

Iterative cone algorithms:

Jet defined as energy flow within a cone of radius R in (y,ϕ) or (η,ϕ) space:

$$R = \sqrt{(y - y_0)^2 + (\phi - \phi_0)^2}$$

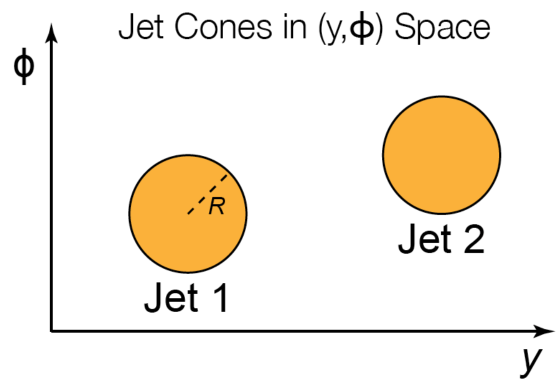

Sequential recombination algorithms:

Define distance measure d_{ij} ...

Calculate d_{ij} for all pairs of objects ...

Combine particles with minimum d_{ij} below cut ...

Stop if minimum d_{ij} above cut ...

e.g. k_T-algorithm:
[see later]

$$d_{ij} = \min\left(k_{T,i}^2, k_{T,j}^2\right) \frac{\Delta Rij}{R}$$

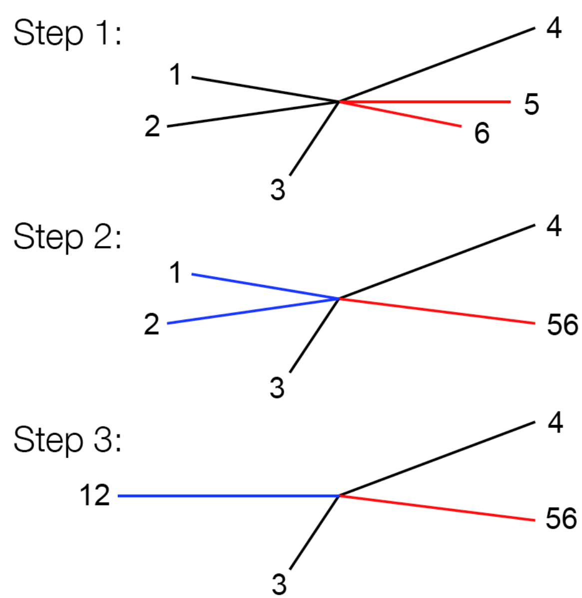

Sequential recombination

Jet energy calibration

Absolute calibration

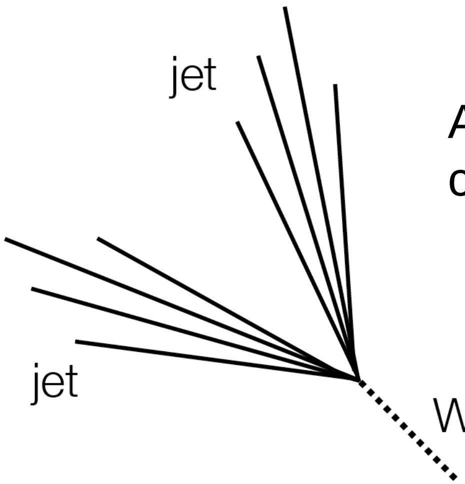

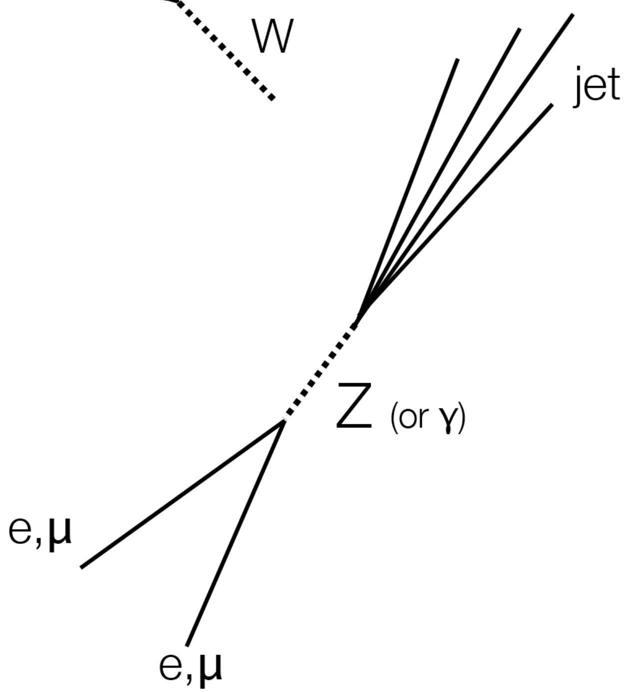

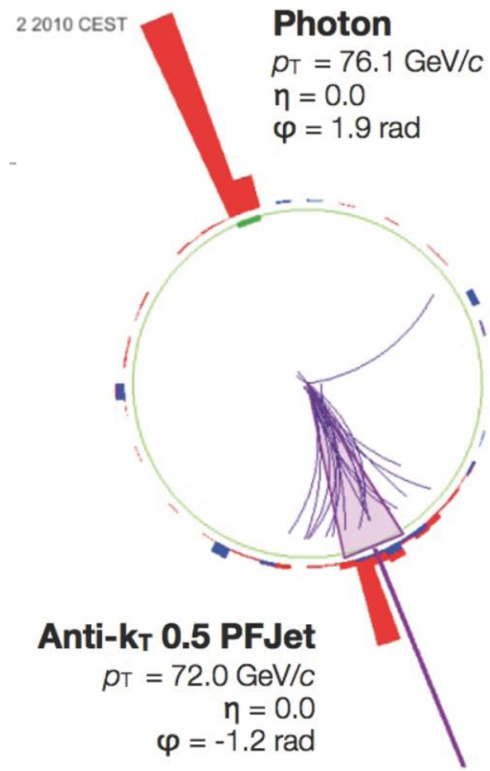

Relative calibration

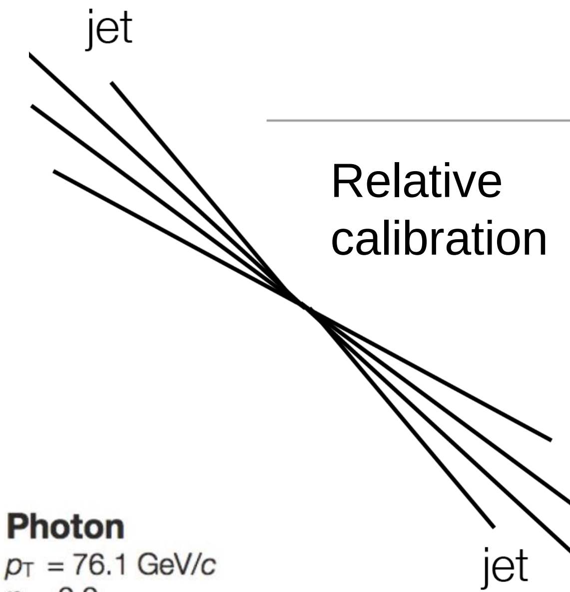

Jet energy resolution

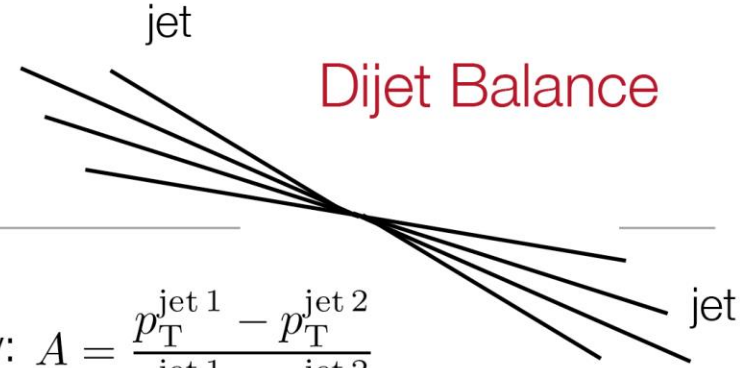

Resolution: $\frac{\sigma(p_T)}{p_T} = \sqrt{2}\sigma_A$ using p_T asymmetry: $A = \frac{p_T^{\text{jet 1}} - p_T^{\text{jet 2}}}{p_T^{\text{jet 1}} + p_T^{\text{jet 2}}}$

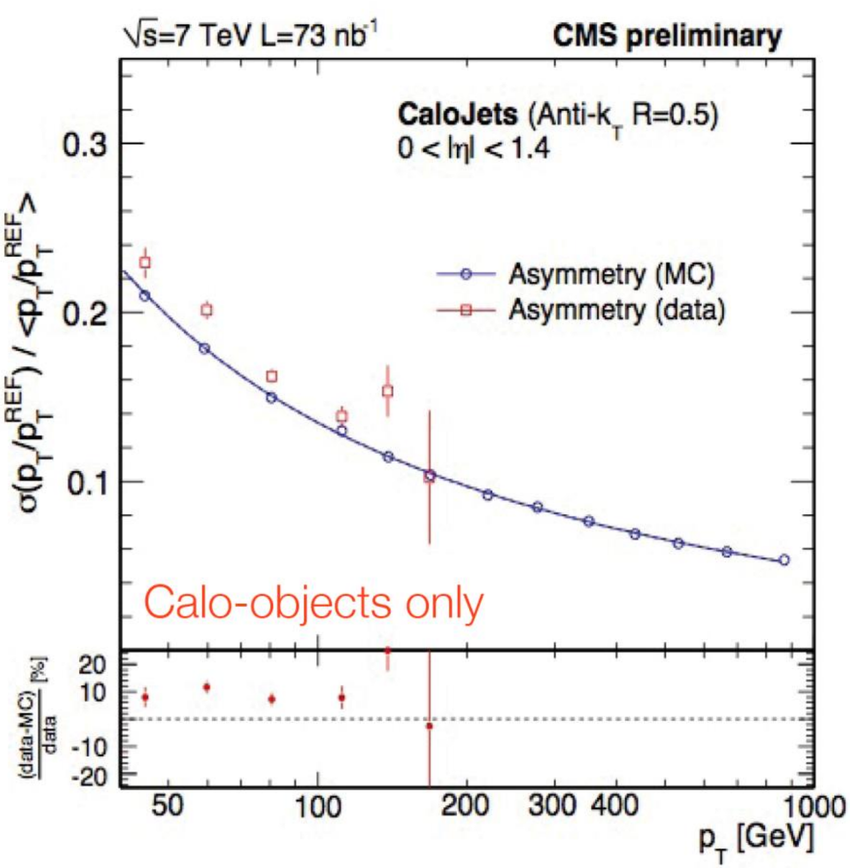

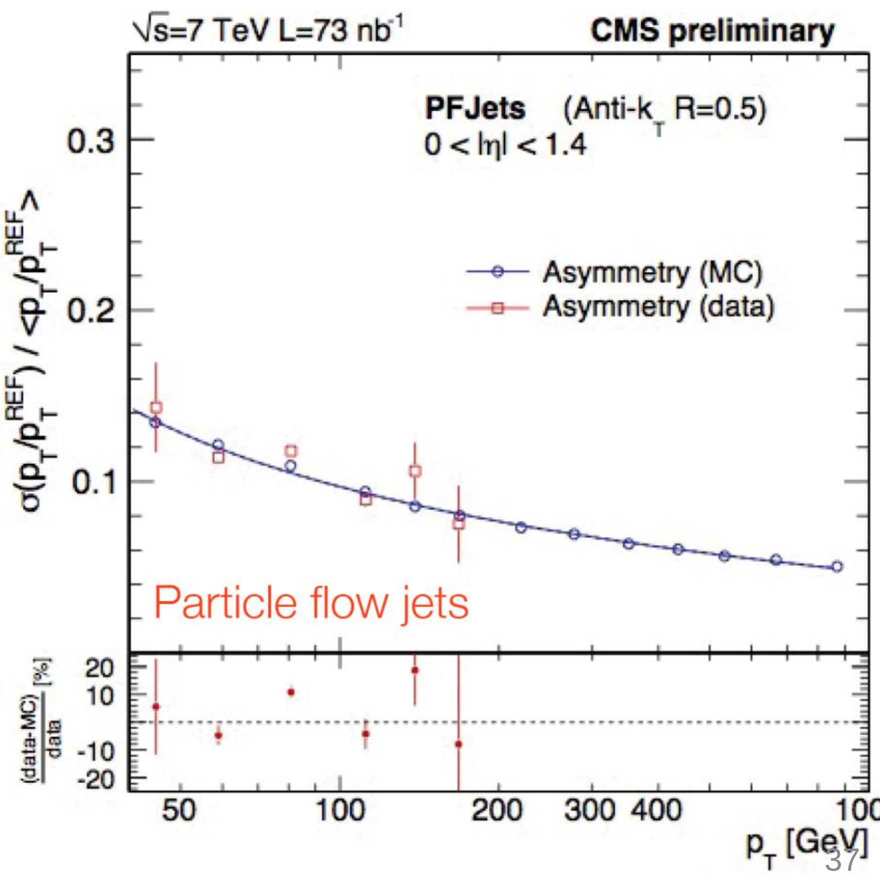

Resolution unfolding

['bin-by-bin' unfolding]

$$N_{\mathrm{part}} = N_{\mathrm{meas}} \cdot \frac{N^{\mathrm{MC}}_{\mathrm{part}}}{N^{\mathrm{MC}}_{\mathrm{meas}}}$$

Measured spectrum =
Real spectrum □ Experim. resolution

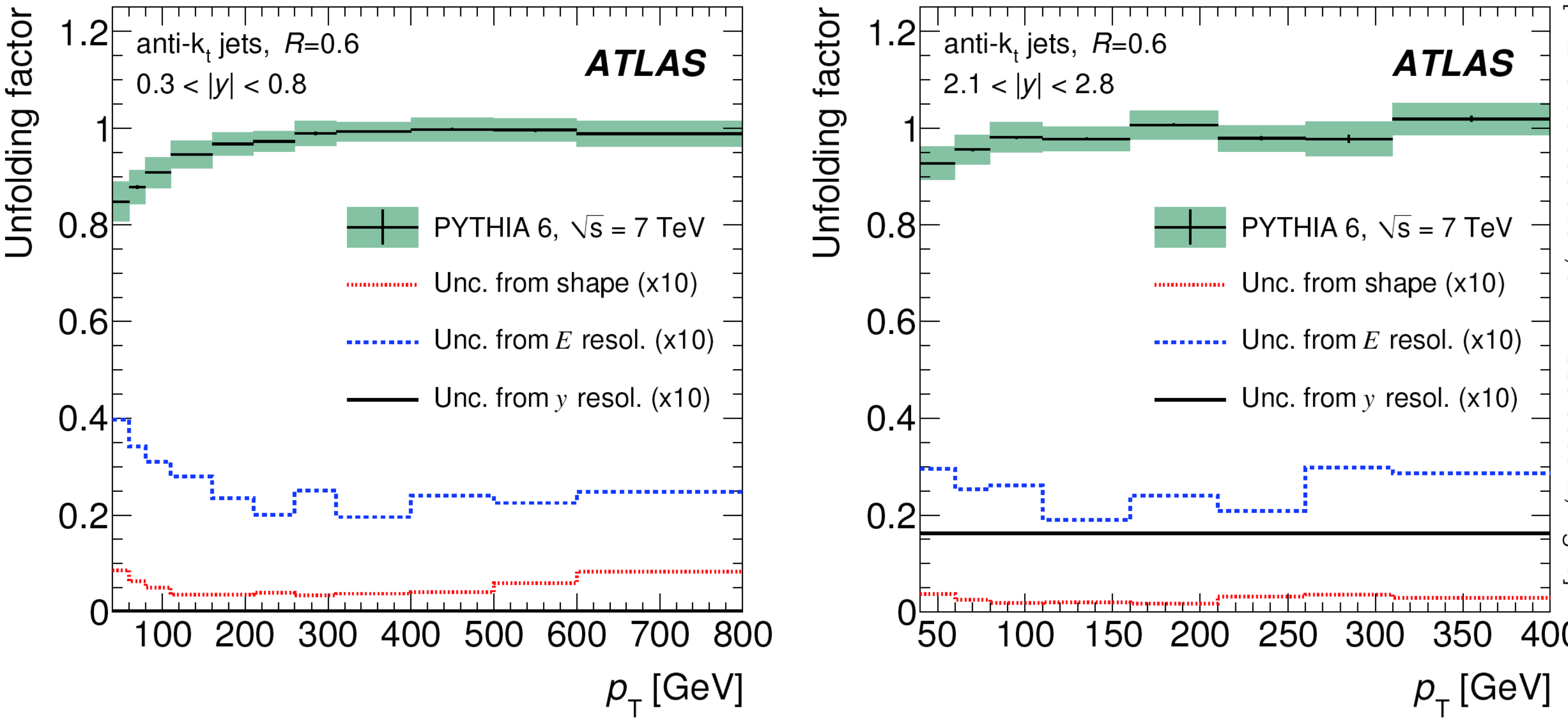

[ATLAS Collaboration; arXiv:1009.5908v2; Fig. 8]

Inclusive jet cross-section

Cross section is huge
(~ Tevatron x 100)

Very good agreement with NLO QCD over nine orders of magnitude

PT extending from 20 to 500 GeV

Main uncertainty:
Jet Energy Scale (3-4%)

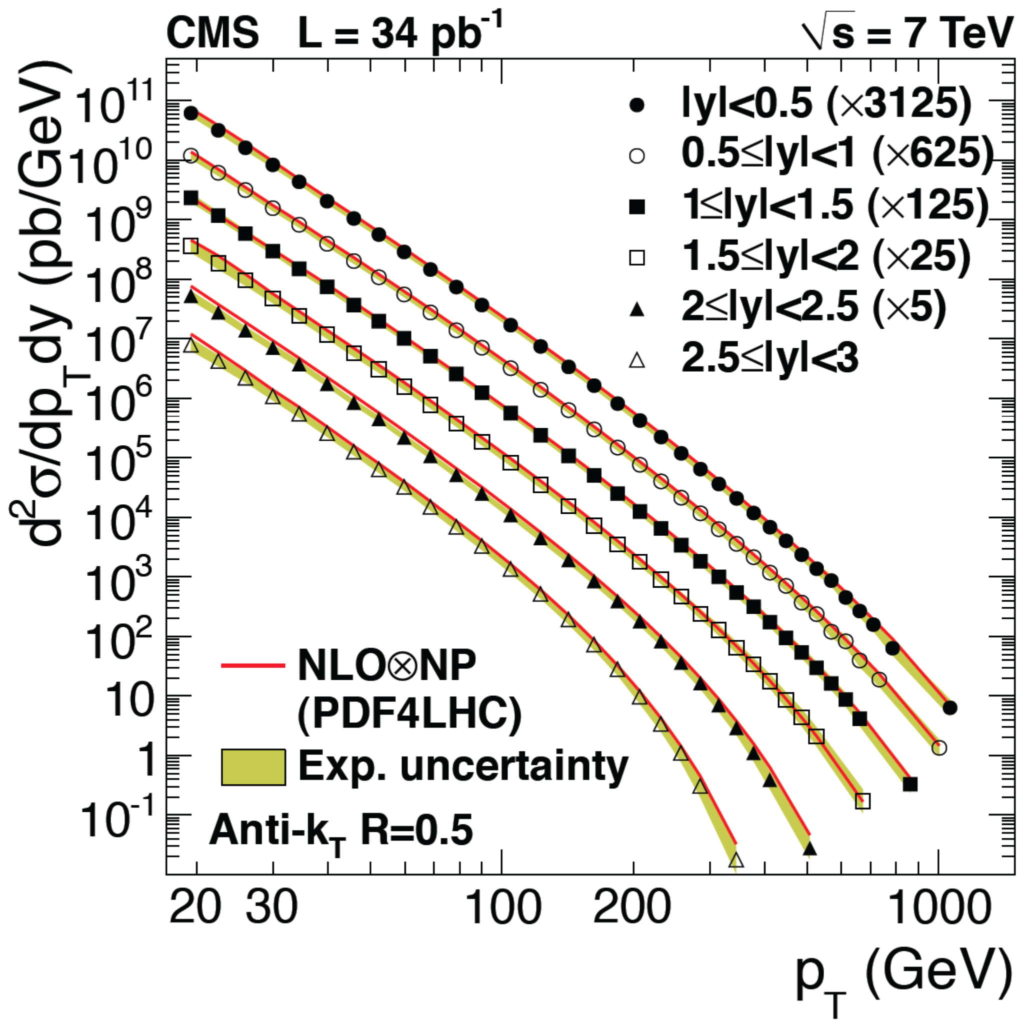

Inclusive jet cross sections: 3-jet / 2-jet ratio

hep-ex 1106.0647, PLB 702 (2011) 336

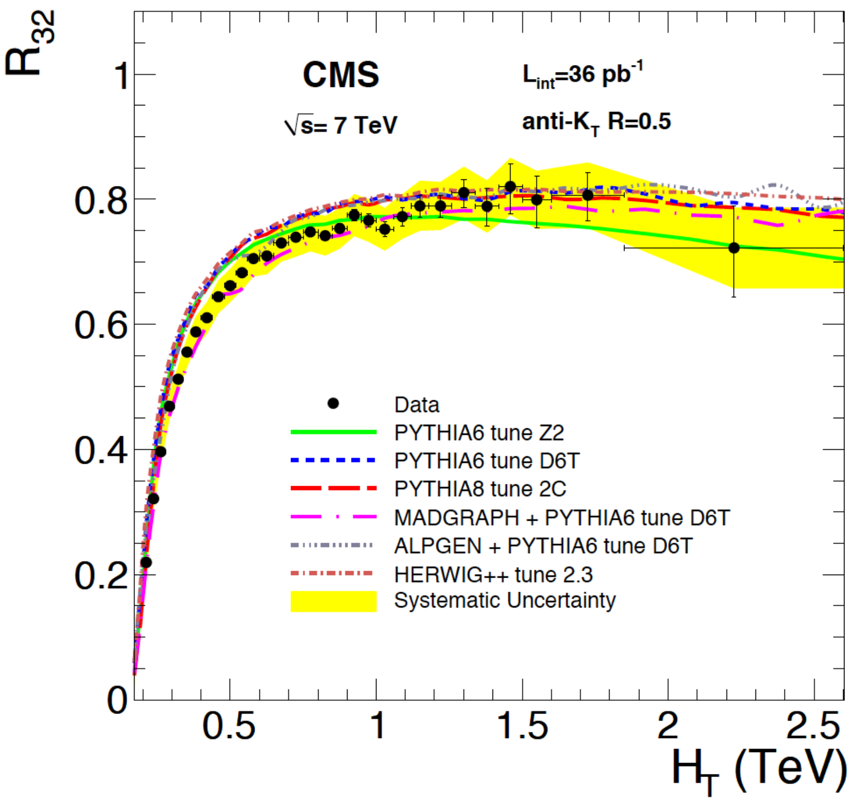

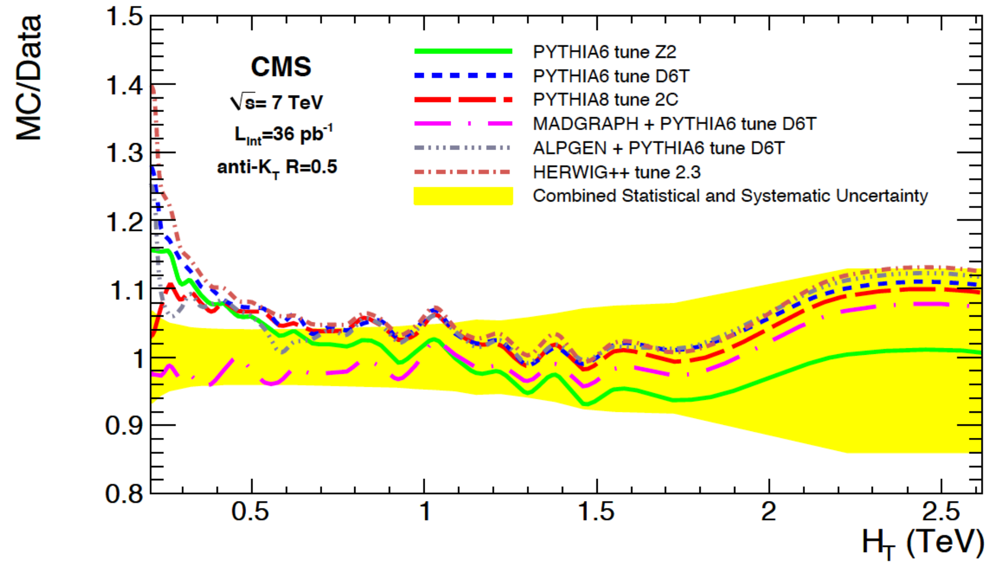

$$H_T = \sum_{i=1}^{N} p_{T\,i}$$

Jets: angular correlations

Difference in azimuth of the two leading jets
Probe of QCD high-order processes
Very slight dependence on JES
No dependence on luminosity

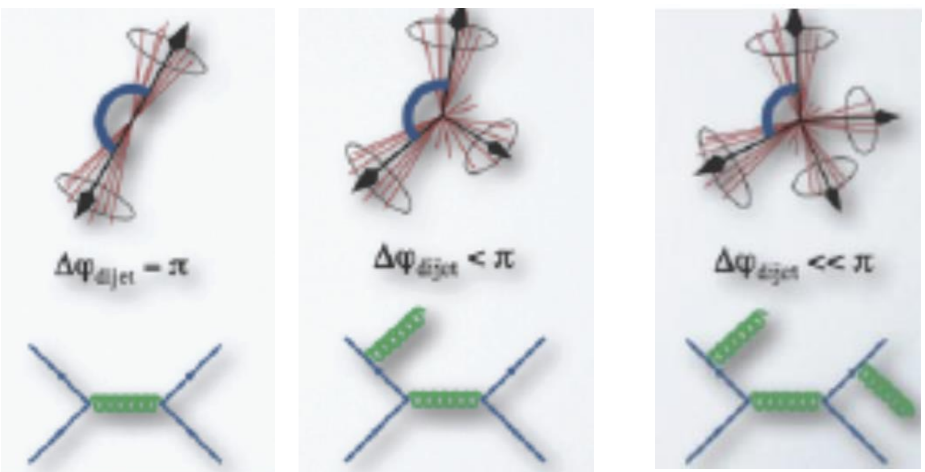

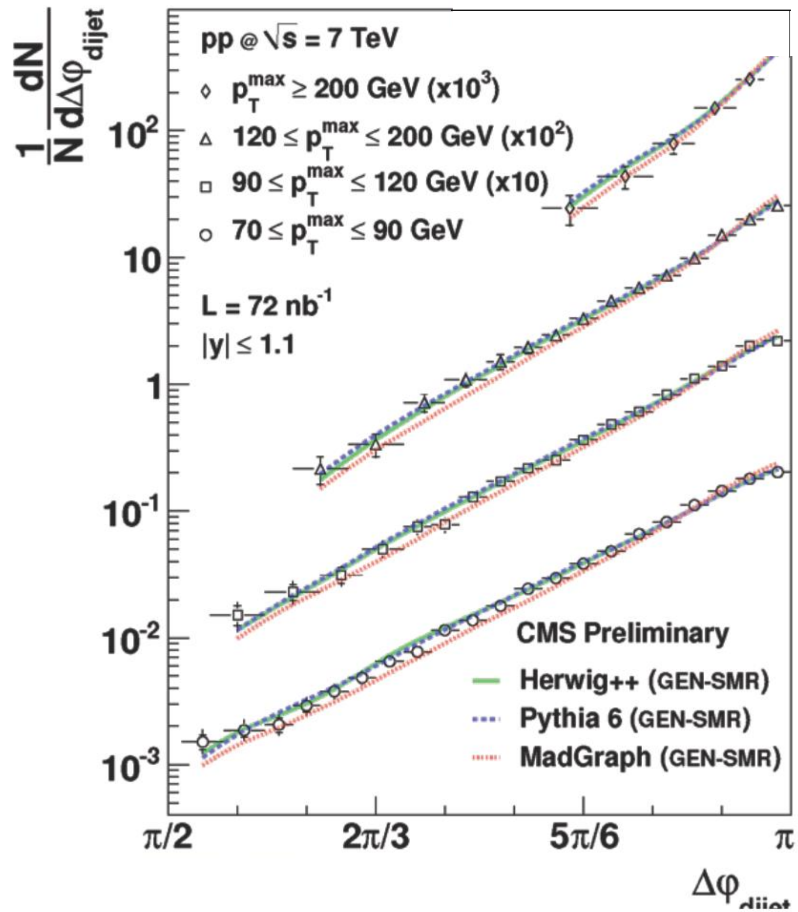

Dijet mass

Very early search for numerous resonances BSM:
string resonance, excited quarks, axi-gluons, colorons, E6 diquarks, W' and Z', RS gravitons

Four-parameter fit to describe QCD shape:

$$\frac{d\sigma}{dm} = p_0 \frac{\left(1 - \frac{m}{\sqrt{s}}\right)^{p_1}}{\left(\frac{m}{\sqrt{s}}\right)^{B}};$$

$$B = p_2 + p_3\left(m/\sqrt{s}\right)$$

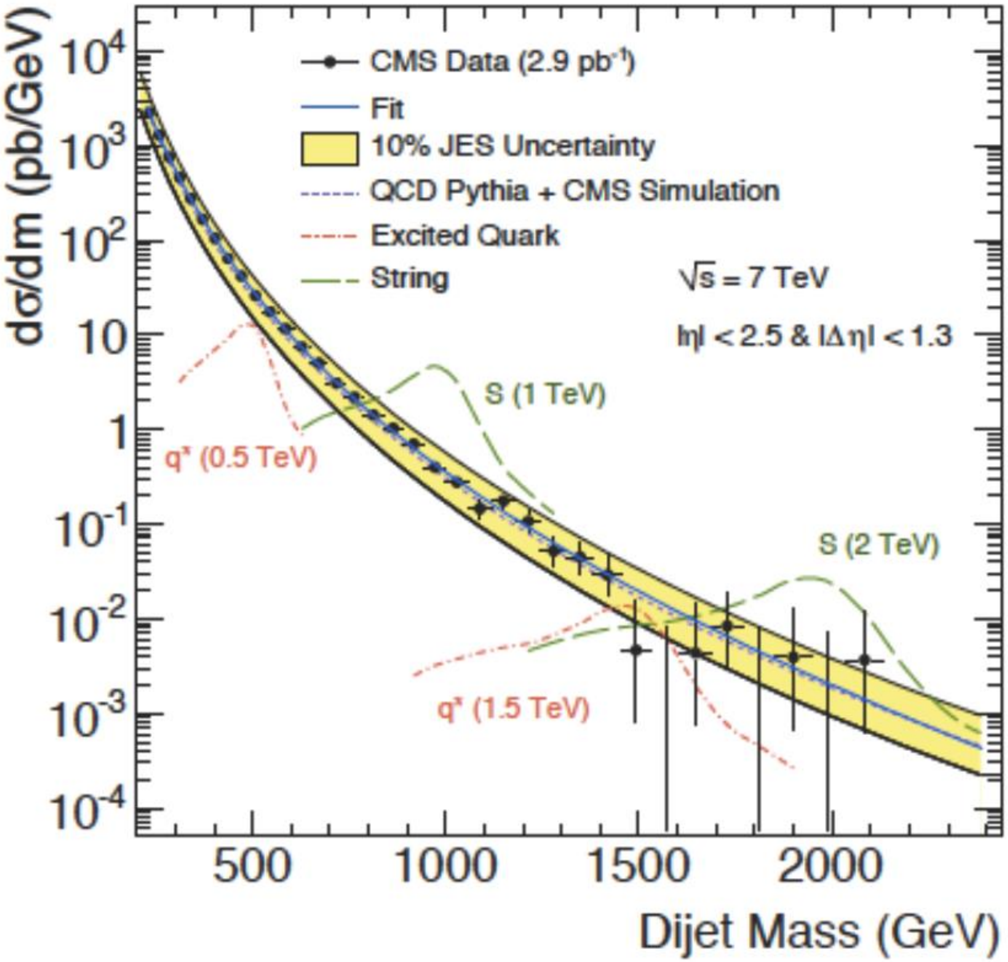

W and Z bosons

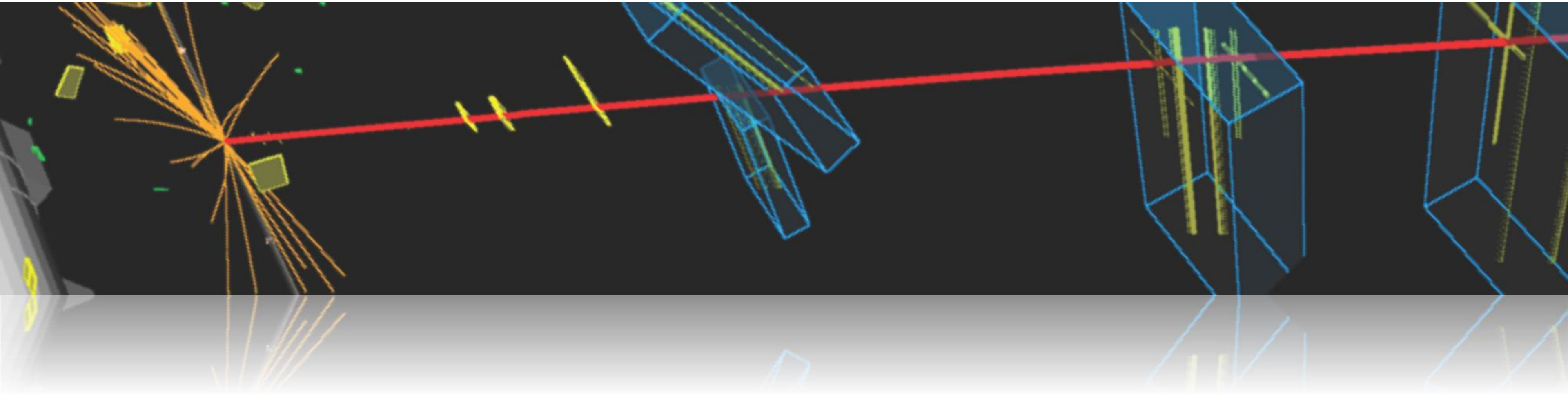

Vector boson production

Direct γ-production:

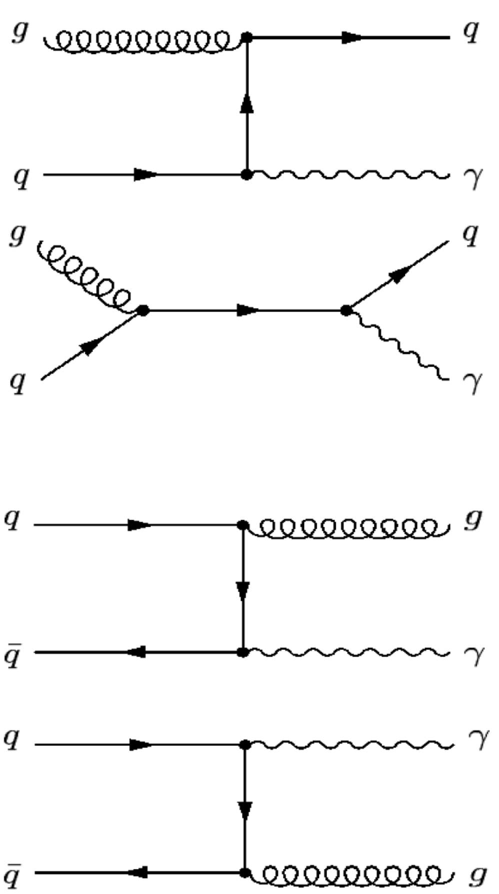

Singel W/Z production:

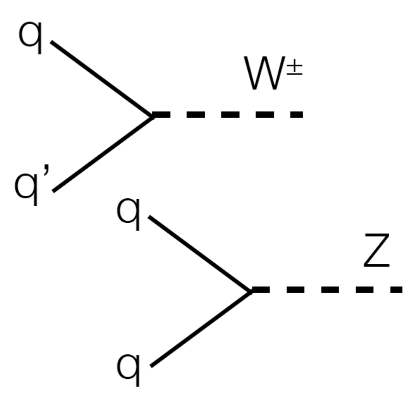

W production:
(main contributions)

$$\begin{cases} u\bar{d} \to W^{+} \\ d\bar{u} \to W^{-} \end{cases}$$

Z production:
(main contributions)

$$\begin{cases} u\bar{u} \to Z \\ d\bar{d} \to Z \end{cases}$$

- At LHC energies these processes take place at low values of Bjorken-x
- Only sea quarks and gluons are involved
- At EW scales sea is driven by the gluon, i.e. x-sections dominated by gluon uncertainty

➥ Constraints on sea and gluon distributions

Examples of high-order processes

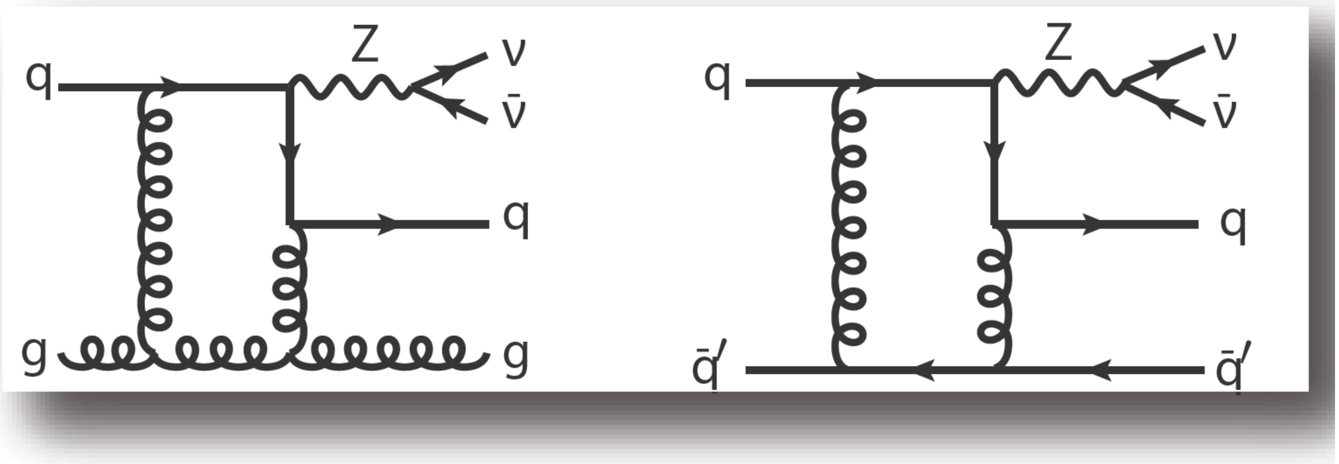

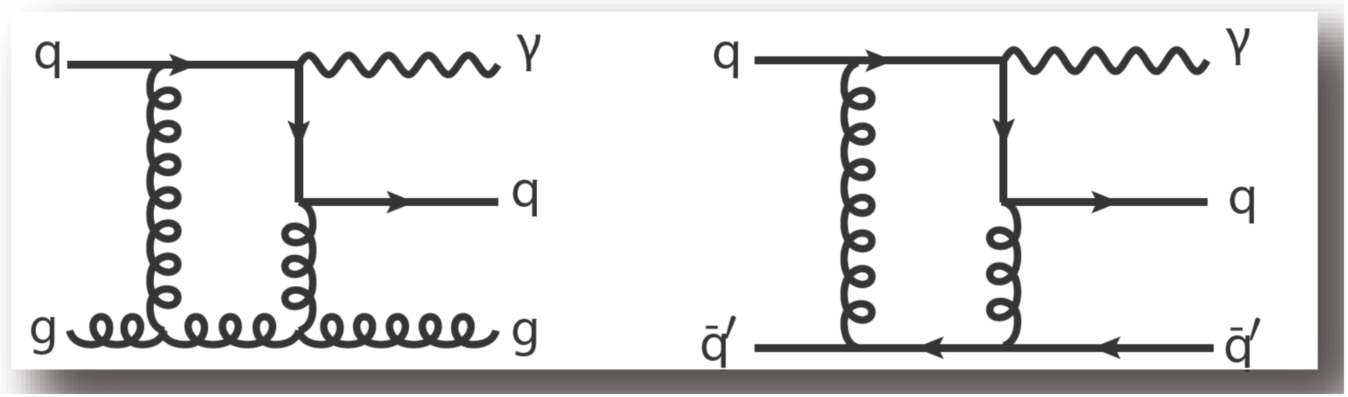

W and Z boson decays

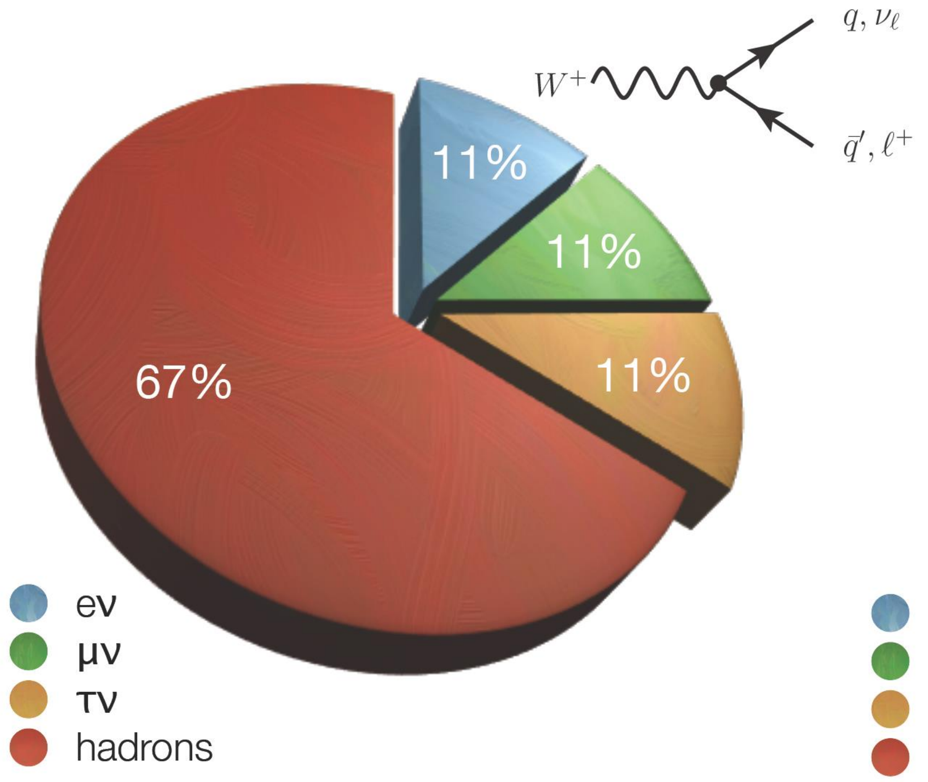

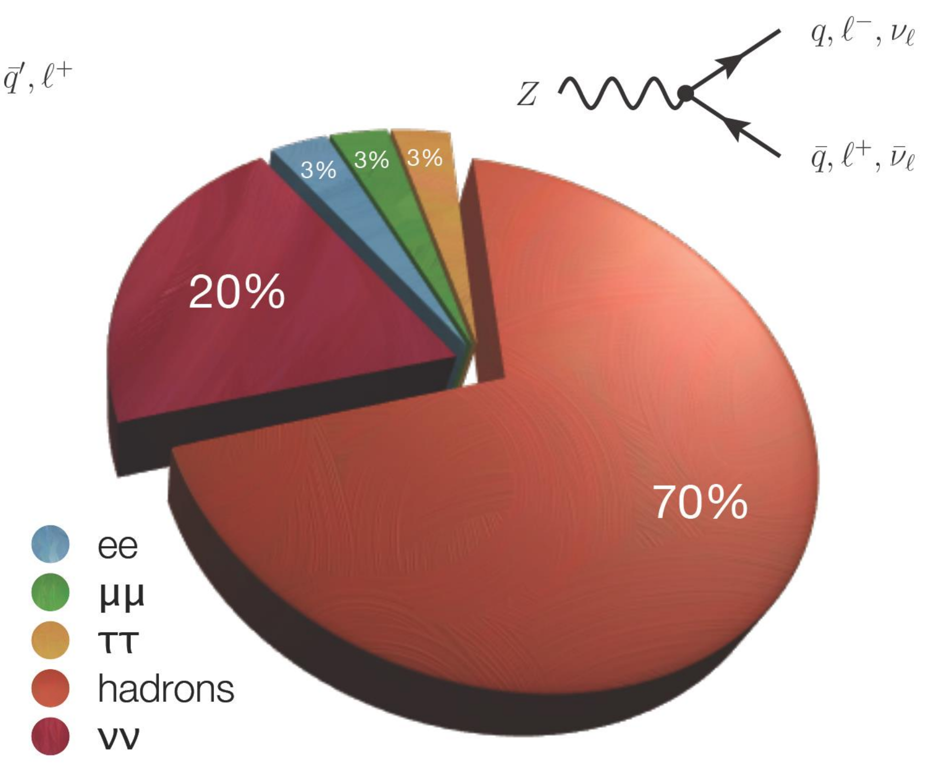

Leptonic decays (e/μ): very clean, but small(ish) branching fractions
Hadronic decays: two-jet final states; large QCD dijet background
Tau decays: somewhere in between…

W and Z boson signatures

[CERN-OPEN-2008-020]

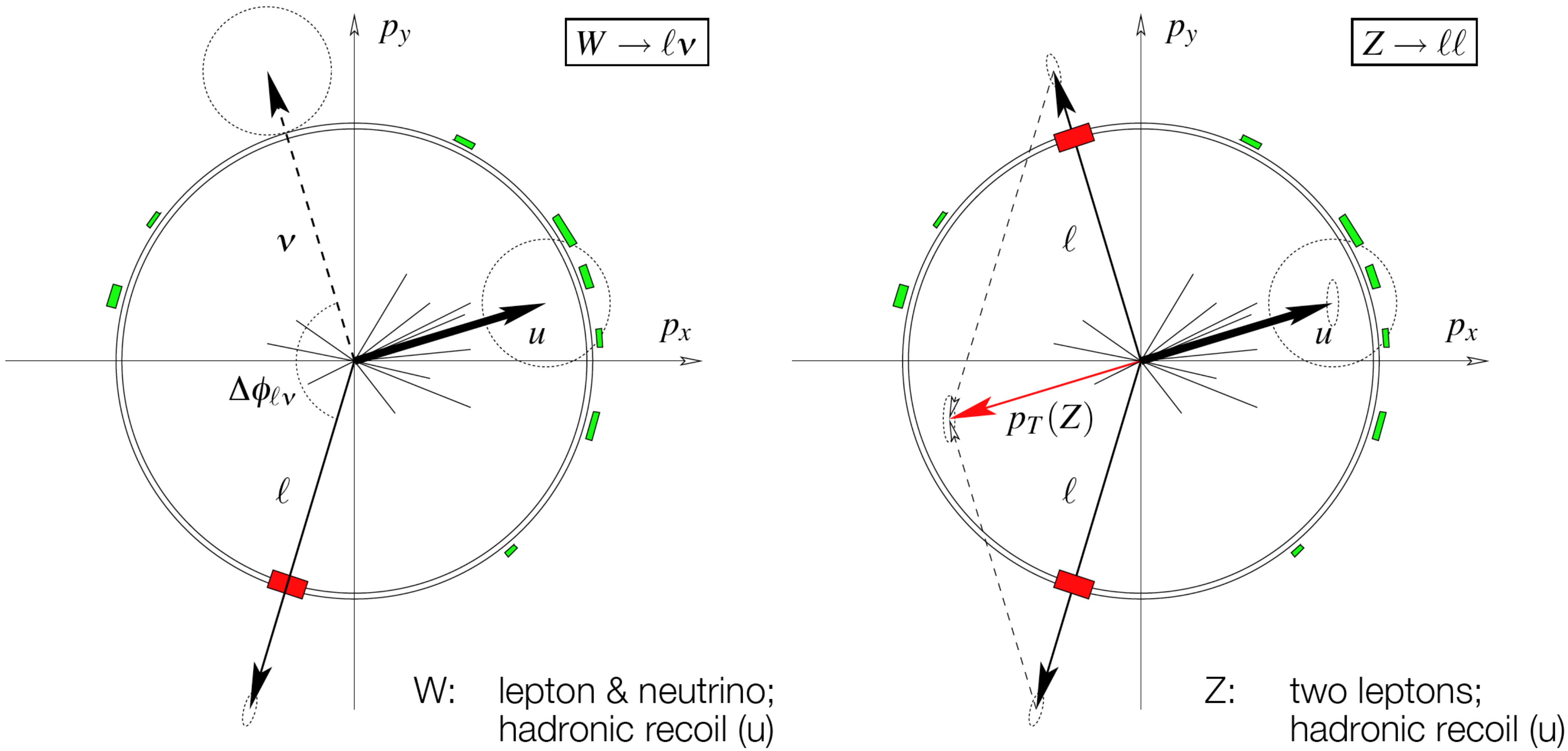

Additional hadronic activity ➛ recoil, not as clean as e^+e^-
Precision measurements: only leptonic decays

Isolated High-p_T Leptons

Starting point for many hadron collider analyses:
isolated high-p_T leptons ➛ discriminate against QCD jets ...

QCD jets can be mis-reconstructed
as leptons ("fake leptons")

QCD jets may contain real leptons
e.g. from semileptonic B decays [$B \rightarrow l\nu X$]

➛ soft and surrounded by other particles

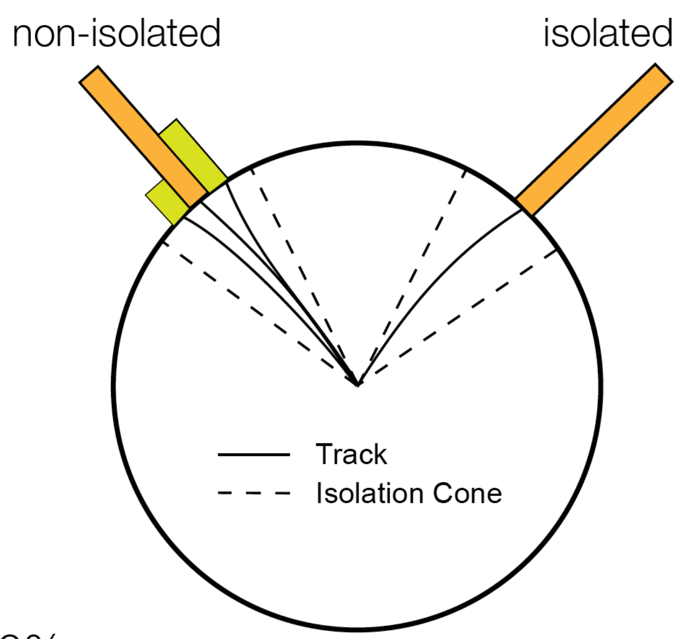

"Tight" lepton selection ...

Require e/μ with p_T > (at least) 20 GeV
Track isolation, e.g. $\sum p_T$ of other tracks
in cone of ΔR=0.1 less than 10% of lepton p_T

Calorimeter isolation, e.g. energy deposition
from other particles in cone of ΔR=0.2 less than 10%

Dilepton mass spectrum at 7 TeV

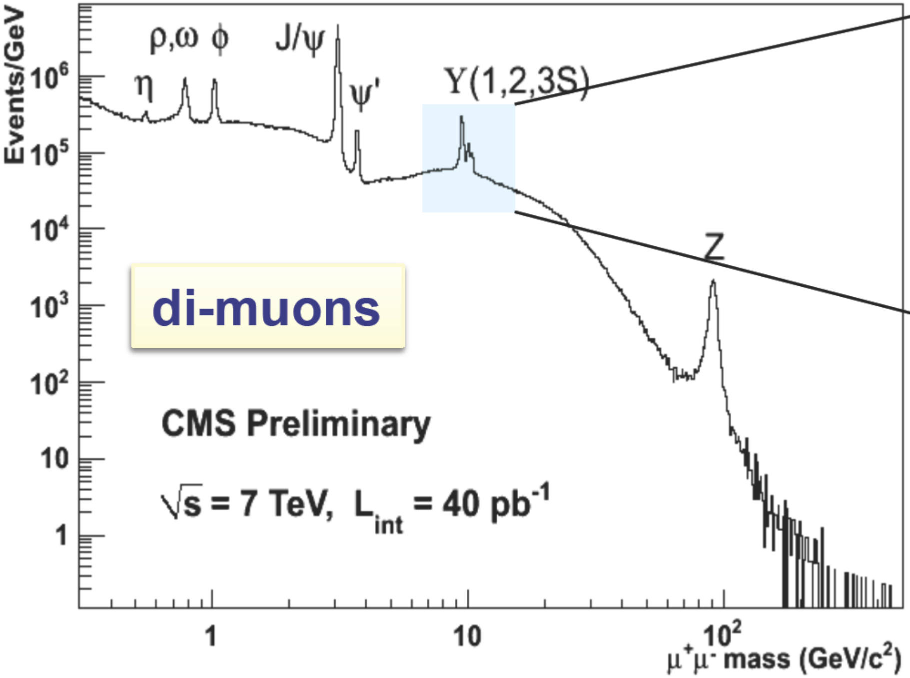

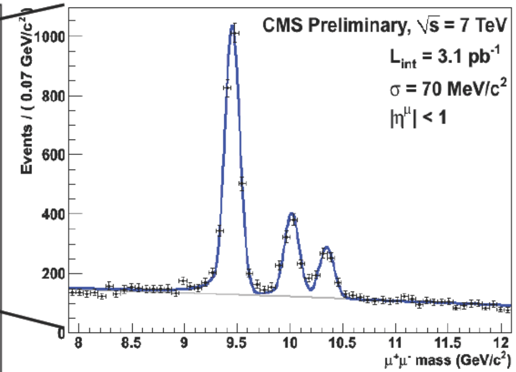

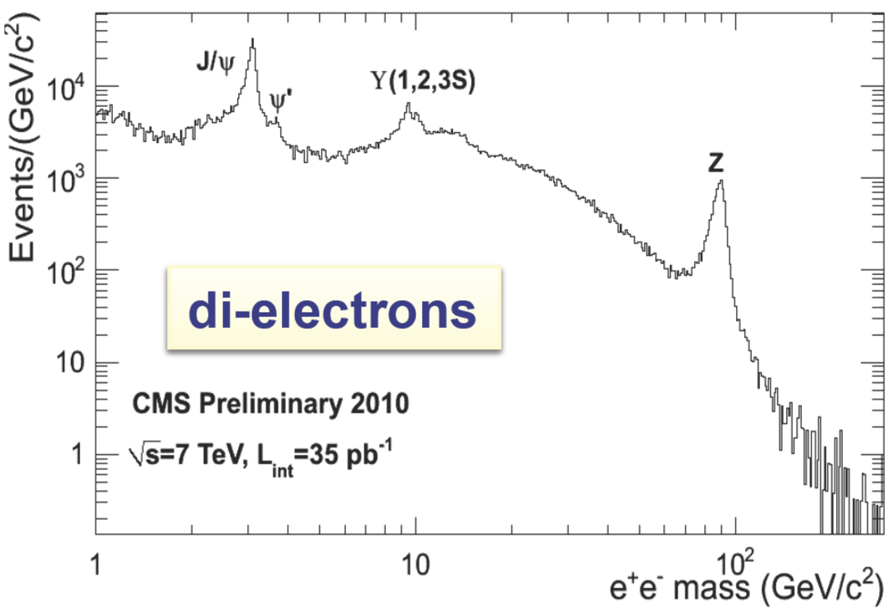

Example: CMS W Analysis

Select isolated electrons and muons ...
[muons: p_T>9 GeV; electrons: p_T>20 GeV]

Investigate transverse mass ...
[Use $E_{T,miss}$; $M_T = (p_{lep} + E_{T,miss})^{½}$]

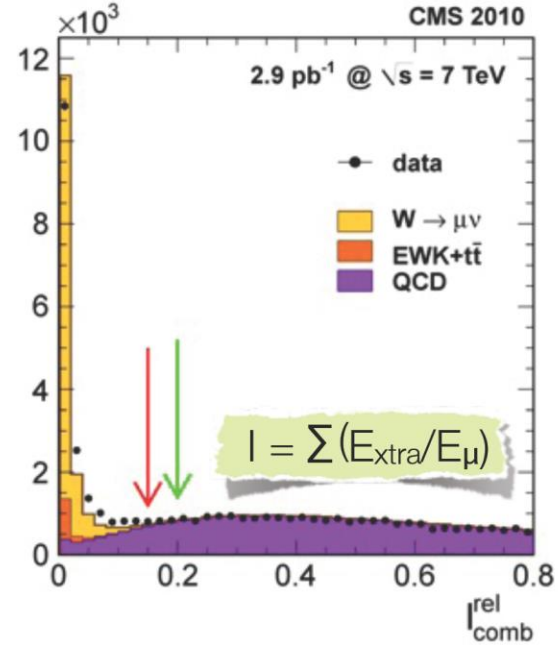

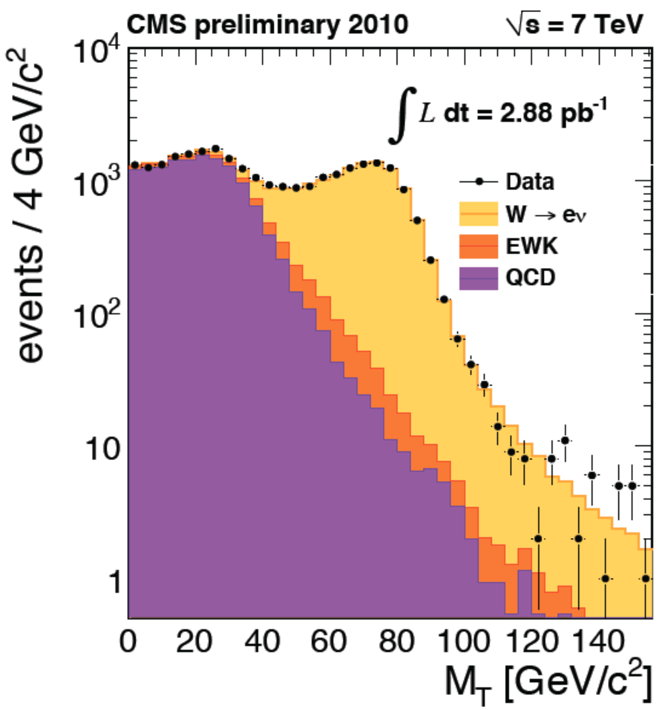

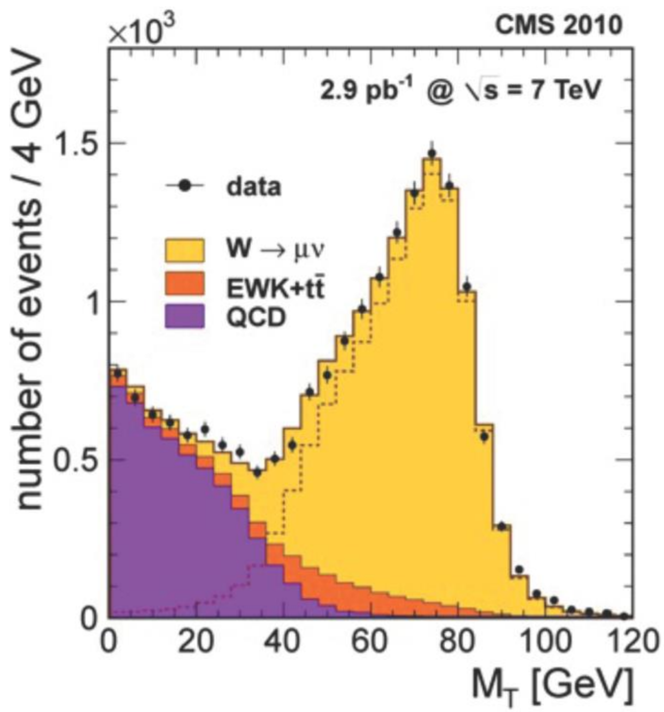

The W signal yield is extracted from a binned likelihood fit to the M_T distribution. Three different contributions:

- W signal
- QCD background
- other (EWK) backgrounds.

W/Z production at 7 TeV

electron(s) | muon(s) | tau(s)

Z Boson

W Boson

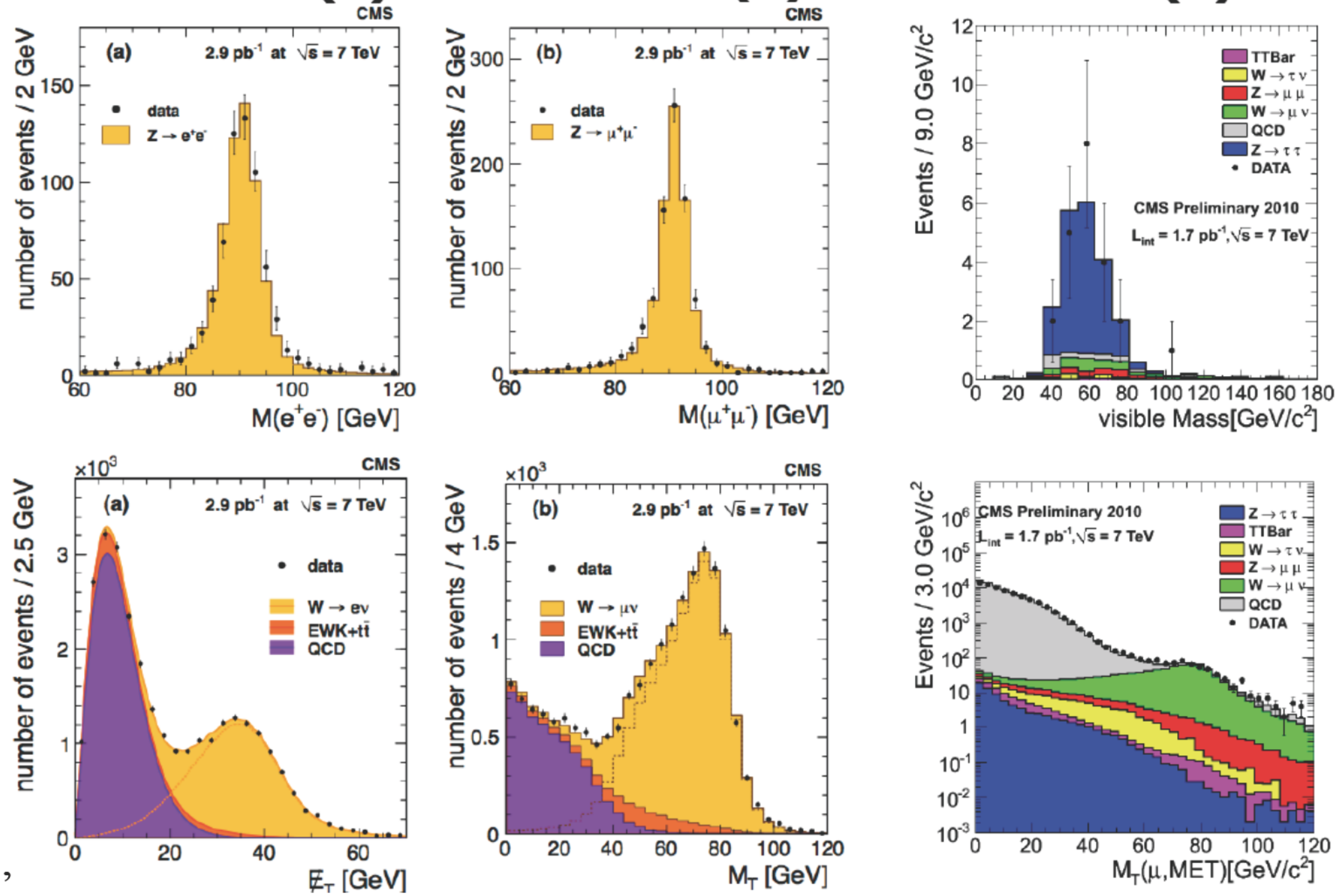

Transverse Mass,

$$M_T = \sqrt{2E_T^{\mu}E_T^{miss}(1-\cos\Delta\phi_{e,miss}}$$

W, Z cross-section v.s. √s

hep-ex 1012.2466, JHEP 01 (2011) 080

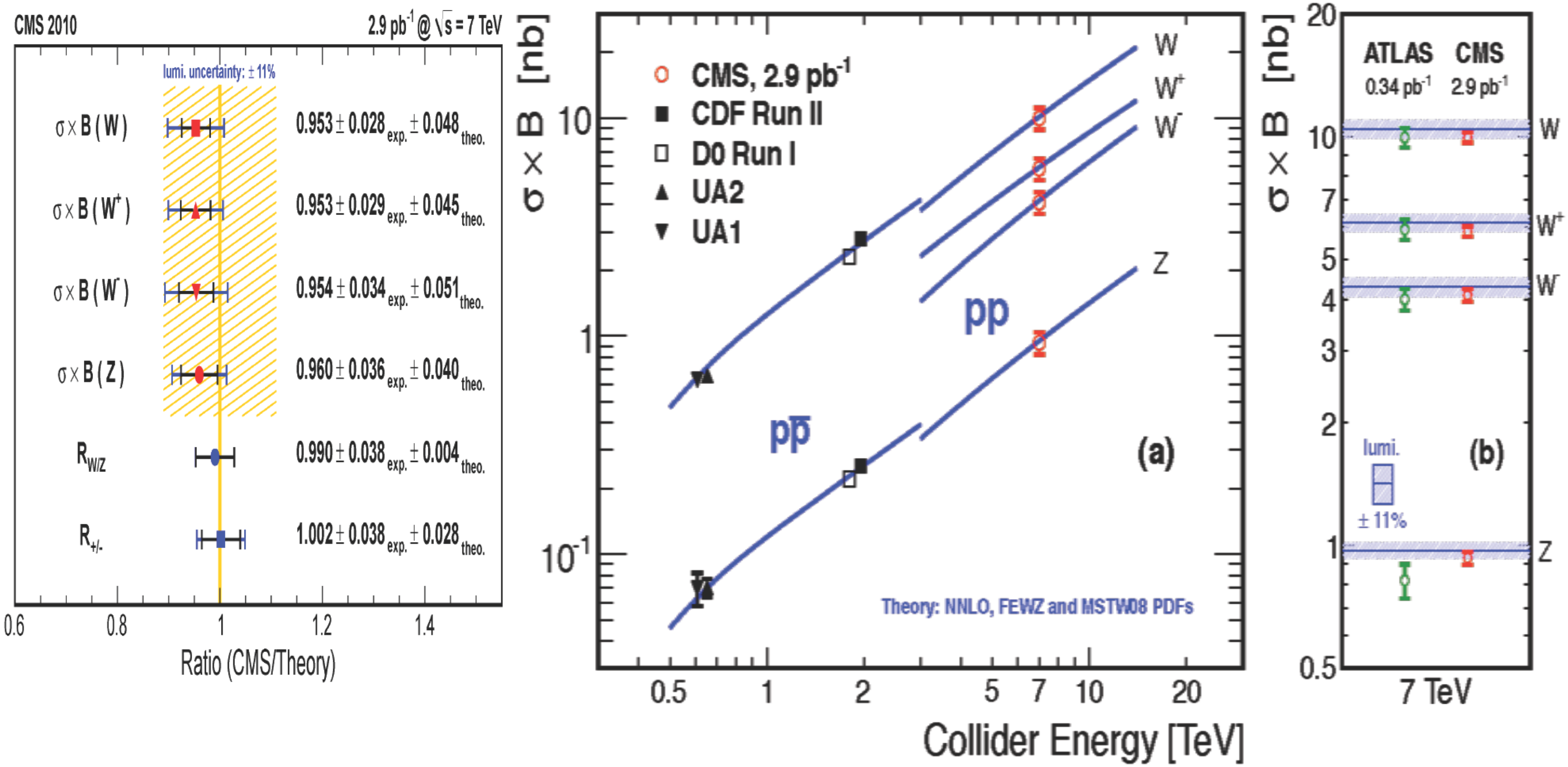

W+/W- charge asymmetry

NNLO cross sections:
scale uncertainties very small

W rapidity: asymmetry
[sensitivity to PDFs]

$$A_W(y) = \frac{d\sigma(W^+)/dy - d\sigma(W^-)/dy}{d\sigma(W^+)/dy + d\sigma(W^-)/dy}$$

Proton-Proton Collider:

symmetry around y=0 ...

PDFs:

u(x) > d(x) for large x ...
more W^+ at positive rapidity

d/u ratio < 1 ...
always more W^+ than W^-

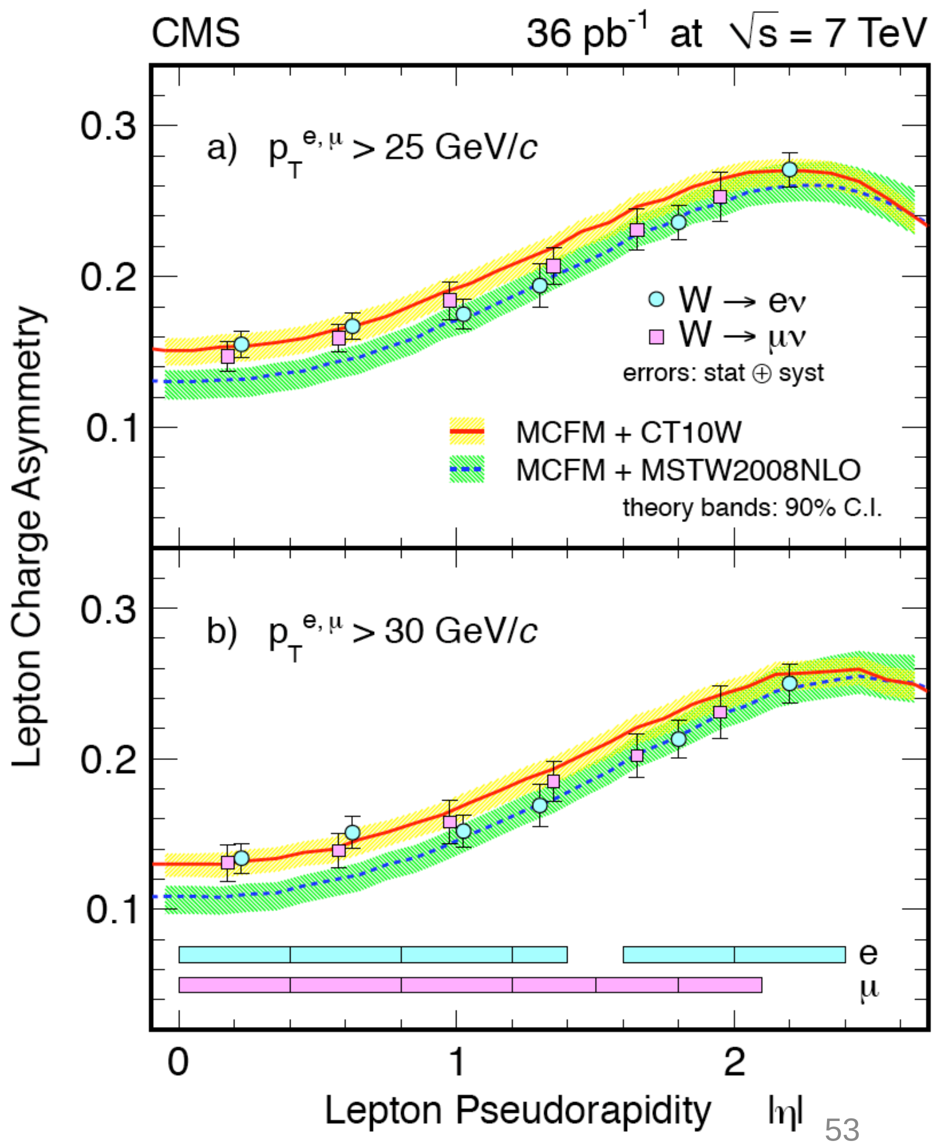

W + Jets multiplicity

$|\eta| < 2.8$ and $p_T > 20$ GeV

arXiv:1012.5382

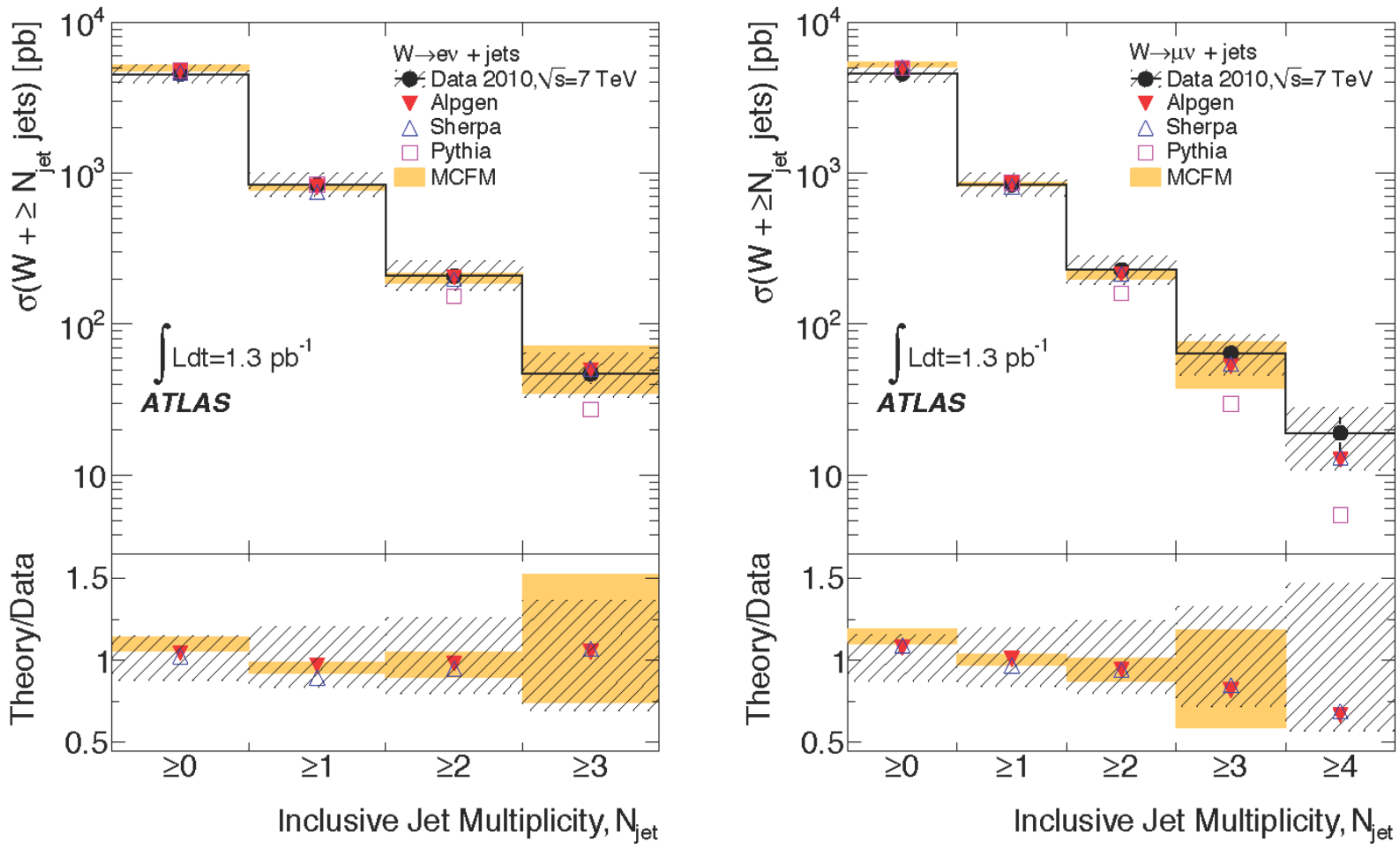

W + Jets P_T

Tails are important in several Exotica and SUSY searches

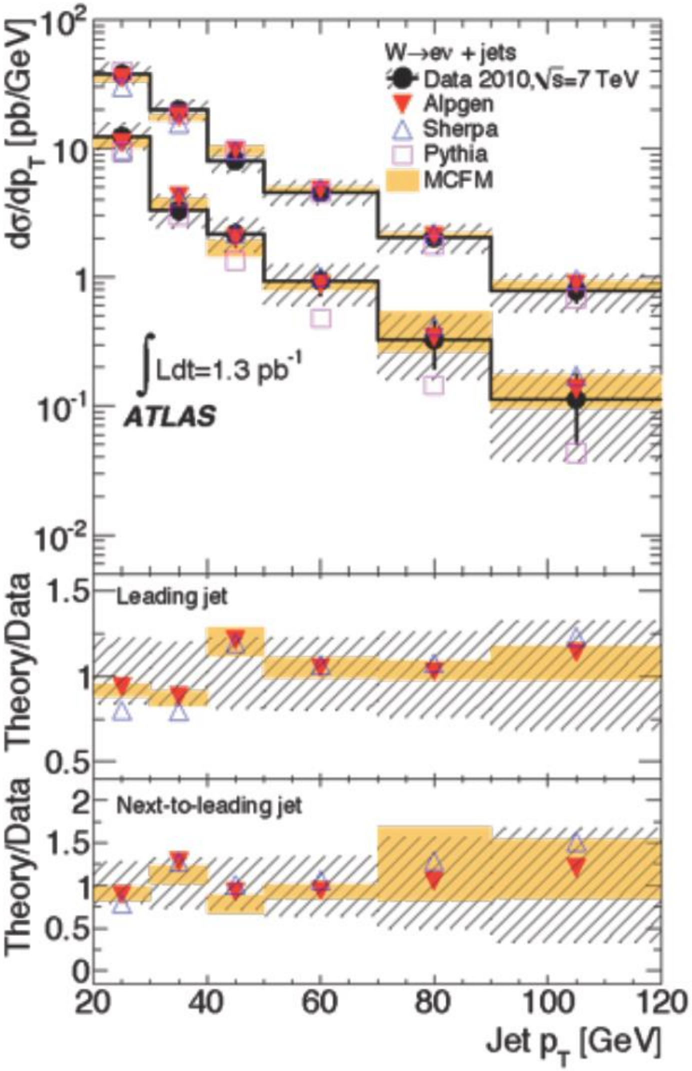

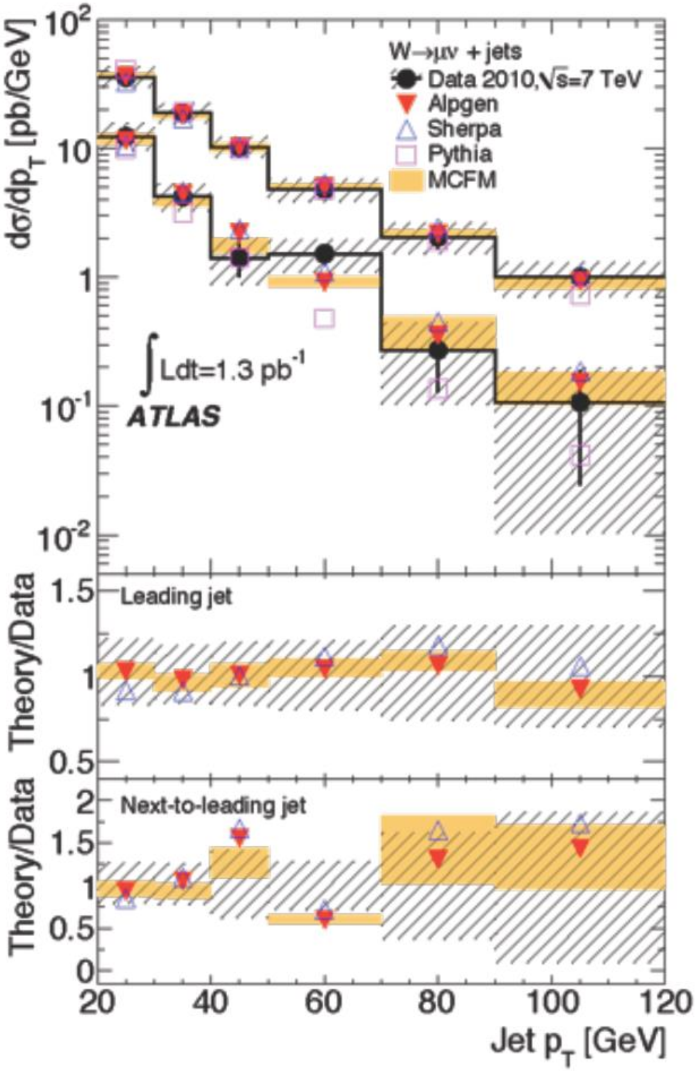

SM processes measured at LHC

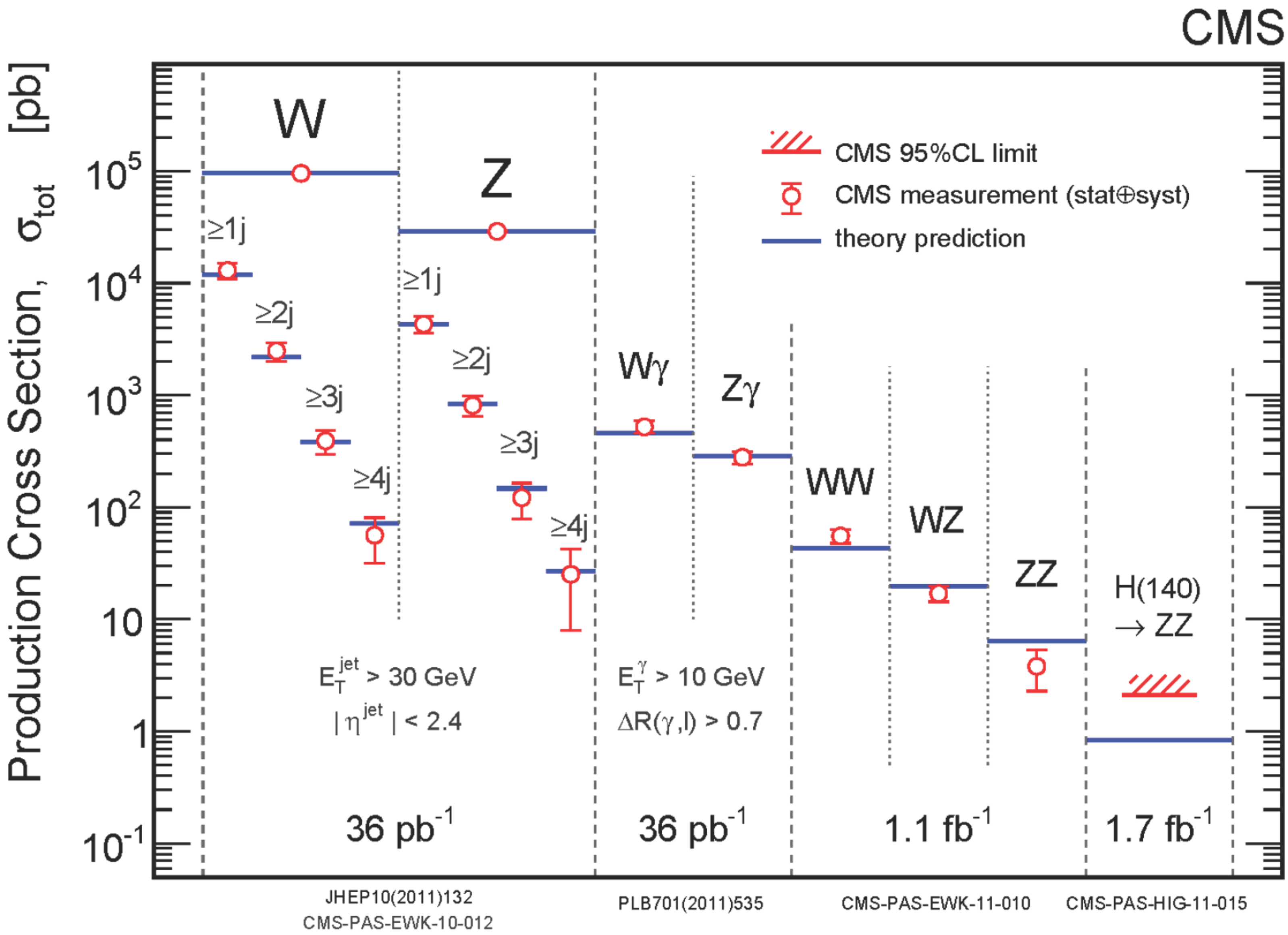

W Mass Determination

Very challenging measurement

Template method:

Fit templates (from MC simulation) with different m_W to data

➛ W mass from best fit

Requires very good modeling of physics & detector

Present
systematic uncertainties:
[DØ-Experiment]

Lepton energy scale: 34 MeV

➛ calibrated to known Z mass
[calorimeter: 3.6% for 50 GeV]

Hadronic recoil: 6 MeV

W production model [PDFs, ...]: 12 MeV

Templates for
m_W = 80.4 ± 1.6 GeV

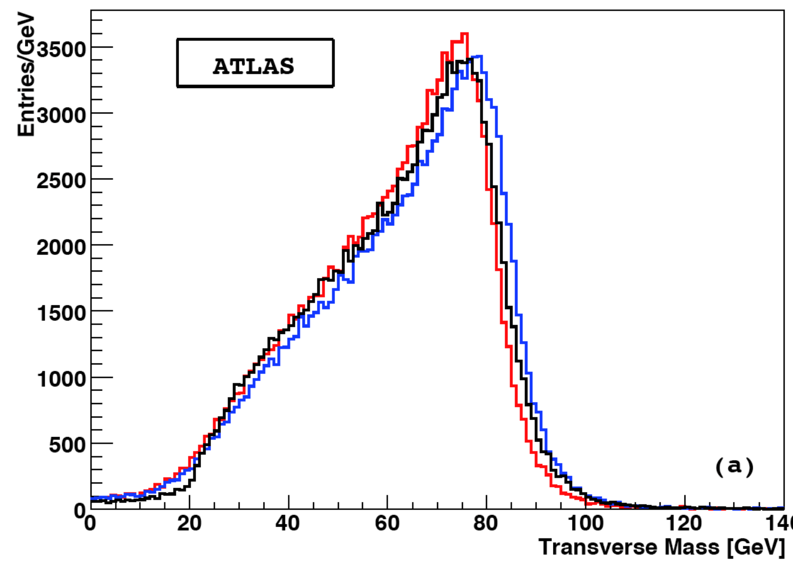

[CERN-OPEN-2008-020]

Ultimate LHC goal:
m_W uncertainty of 15 MeV
[via combination]

End of Lecture 3